Journal of Materials Research and Technology 30 (2024) 3308–3327

Contents lists available at ScienceDirect

Journal of Materials Research and Technology

journal homepage: www.elsevier.com/locate/jmrt

Development of ultra-lightweight foamed concrete modified with silicon dioxide (SiO_2) nanoparticles: Appraisal of transport, mechanical, thermal, and microstructural properties

Samadar S. Majeed [a], Md Azree Othuman Mydin [b,**], Alireza Bahrami [c,*], Anmar Dulaimi [d,e], Yasin Onuralp Özkılıç [f,g], Roshartini Omar [h], P. Jagadesh [i]

[a] Civil Engineering Department, College of Engineering, Nawroz University, Duhok, Kurdistan Region, Iraq
[b] School of Housing, Building and Planning, Universiti Sains Malaysia, Penang, 11800, Malaysia
[c] Department of Building Engineering, Energy Systems and Sustainability Science, Faculty of Engineering and Sustainable Development, University of Gävle, 801 76 Gävle, Sweden
[d] Department of Civil Engineering, College of Engineering, University of Kerbala, Karbala, 56001, Iraq
[e] College of Engineering, University of Warith Al-Anbiyaa, Karbala, 56001, Iraq
[f] Department of Civil Engineering, Faculty of Engineering, Necmettin Erbakan University, 42100, Konya, Turkey
[g] Department of Civil Engineering, Lebanese American University, Byblos, Lebanon
[h] Department of Construction Management, Faculty of Technology Management and Business, Universiti Tun Hussein Onn Malaysia, Parit Raja, Batu Pahat, Johor, 86400, Malaysia
[i] Department of Civil Engineering, Coimbatore Institute of Technology, Tamil Nadu, 638 056, India

ARTICLE INFO

Handling editor: Prof. M Meyers

Keywords:
Lightweight foamed concrete
Nanoparticles
Silicon dioxide
Compression
Thermal conductivity
Porosity
Intrinsic air permeability
SEM

ABSTRACT

Over the last few decades, researchers have devoted significant consideration to the use of nanoscale elements in concrete. Silicon dioxide nanoparticles (SDNs) have been a popular subject of study among the several types of nanoparticles. This article describes the findings of a laboratory investigation that examined the properties of ultra-lightweight foamed concrete (ULFC) including different proportions of SDNs. Wide range of the properties was evaluated specifically the slump flow, density, consistency, flexural strength, modulus of elasticity, compressive strength, split tensile strength, thermal properties, porosity, water absorption, sorptivity, intrinsic air permeability, and chloride diffusion. Additionally, the scanning electron microscopy (SEM) and pore distributions analyses of different mixes were done. Results confirmed a noticeable increase in the mechanical properties of ULFC, with respective improvements in the 28-day compressive, split tensile, and flexural strengths of up to 70.49%, 76.19%, and 51.51%, respectively, at 1.5% of the SDNs inclusion. However, further increases in the SDNs percentage did not result in remarkable enhancements. As the SDN percentage increased from 1.5% to 2.5%, the ULFC's sorptivity, porosity, water absorption, intrinsic air permeability, and chloride diffusion showed substantial improvements. When compared to the control sample, ULFC with SDNs demonstrated higher thermal conductivity values. The reason for this occurrence was determined to be the smaller pore size observed in the ULFC specimens containing SDNs. A great adjustment in the distribution of pore diameters was witnessed in the ULFC mixes when the percentages of SDNs were adjusted. The ULFC specimens, which included SDNs at the percentages of 0.5%, 1.0%, and 1.5%, indicated a reduction in the total number of large voids measuring 500 nm or more, compared to the control ULFC specimen. The findings of this study highlight the potential benefits of incorporating SDNs into ULFC, which may improve its overall properties.

* Corresponding author.
** Corresponding author.
E-mail addresses: Samadar.salim@nawroz.edu.krd (S.S. Majeed), azree@usm.my (M.A. Othuman Mydin), alireza.bahrami@hig.se (A. Bahrami), yozkilic@erbakan.edu.tr (Y.O. Özkılıç), shartini@uthm.edu.my (R. Omar), jaga.86@gmail.com (P. Jagadesh).

https://doi.org/10.1016/j.jmrt.2024.01.282
Received 22 December 2023; Received in revised form 22 January 2024; Accepted 30 January 2024
Available online 6 February 2024

1. Introduction

Concrete is widely recognised as a vital construction material that holds significant importance in both residential and commercial building projects, as well as recent engineering structures on a global scale. In addition to satisfying the criteria of possessing high compressive and tensile strengths, concrete exhibits favourable attributes such as ease of fabrication, durability, fire resistance, and long-lasting impermeability. In addition, concrete's affordability, availability of constituent materials, and ability to be moulded into a variety of structures are all factors that consistently establish it as the material of choice among construction engineers, notwithstanding its adverse environmental effects [1]. Annually, a staggering quantity of 25 billion metric tonnes of concrete is manufactured [2]. As a result, environmental activists' raise concern regarding the substantial carbon dioxide emissions resulting from the production of cement for concrete, which accounts for approximately 10% of worldwide emissions [3]. However, it is important to acknowledge that concrete does have certain drawbacks, including brittleness, a porous structure, and potential volume volatility [4]. The use of nanotechnology in cement-based materials has generated increasing interest among researchers in recent years [5]. This has been attributed to the enormous potential that nanotechnology holds in this field.

The use of nanomaterials in the production of concrete provides numerous benefits. One notable characteristic of this substance is its ability to function as an activator, thereby augmenting the reactivity of pozzolans. Additionally, it facilitates the early development of strength in mortar and concrete by enhancing the hydration of cement [6]. The addition of nanomaterials to concrete considerably improves its compressive and flexural strengths. Furthermore, the process of concrete pore refinement serves to diminish the chloride penetration, thus effectively thwarting steel corrosion. In addition, research has pointed out that nanomaterials can decrease the level of carbonisation in concrete. Determining the strength of concrete, the interface between the cement matrix and aggregates is subsequently strengthened. Ultimately, the incorporation of nanomaterials into concrete results in an enlargement of calcium hydroxide particles and a heightened propensity for tropism production [7–9]. The techniques strive to be low-pressure, energy-efficient, and non-toxic, thereby fostering ecological sustainability [10,11]. The elevated ratio of surface area to volume signified by the small particulate size expedites the hydration of cement and, ultimately, the pozzolanic reaction [12]. Furthermore, apart from the ecological benefits linked to nanoparticles, their integration holds promise for improving the structural efficacy, longevity, and robustness of cementitious materials [13,14].

Lightweight foamed concrete (LWFC) is a variant of concrete characterised by its low density, typically ranging from 350 to 2000 kg/m^3 [15]. In the case of structural LWFC, the unit weight falls within the range of 1400–2000 kg/m^3, whereas regular weight concrete typically has a unit weight of 2400 kg/m^3 [16]. By decreasing the weight of the structure, itself, buildings can be designed with smaller cross-sectional structural components, resulting in increased efficiency of useable spaces [17]. In recent infrastructure and building construction initiatives, the application of LWFC has become more widespread. All these advantages can be ascribed to its beneficial characteristics, which consist of a decreased self-weight, outstanding resistance to fire, and excellent thermal insulation properties [18]. However, the application of LWFC is impeded by several constraints, such as unfavourable strength properties, high drying shrinkage, and an increased vulnerability to splitting. These factors impede the extensive adoption of LWFC on a global scale [19]. The use of prefabricated foams in LWFC leads to the creation of a multitude of air voids. A close correlation exists between these foams and the strength characteristics, durability attributes, and pore configurations of LWFC [20]. Consequently, incorporating solid additives in nano-sized form during the fabrication process of LWFC can greatly enhance its properties [21]. Within the category of solid particles, it has been observed that silicon dioxide nanoparticles (SDNs) possess a high charge-to-size ratio. Consequently, these SDNs tend to display a prevalence of deprotonated hydroxyl groups on their surface and tend to be absorbed onto positively charged ions of surfactants. On the other hand, alumina particles have a propensity to be adsorbed by surfactants containing carboxyl groups [22]. Previous studies have illustrated that as LWFC's absorption capacity rises, the thickness of the interfacial transition zone (ITZ) tends to decline. This is due to the reduced accumulation of water in the vicinity of the fine aggregate particle [23]. Furthermore, it should be noted that LWFC possesses the inherent benefit of internal curing, which has the potential to mitigate the shrinkage cracking and decrease the permeability, as stated in Ref. [24]. The implementation of SDNs has the potential to noticeably improve the resistance of LWFC against the entry of water and chloride ions, as stated by previous research [25]. The enhancement of the bond at the interface between LWFC is attributed to two factors: improved particle packing at the nanoscale scale and the occurrence of the pozzolanic reaction facilitated by the presence of amorphous silica.

To date, there have been an inadequate number of research undertaken to investigate the possible application of nanoparticles in the manufacture of LWFC. Most of the research conducted thus far has focused on the utilisation of various nanoparticles to boost the properties of normal weight concrete. Of the several nanoparticles under consideration, it has been observed that SDNs are the most extensively used and researched [26]. Silica aerogel, sometimes referred to as SDNs, is a finely powdered substance consisting of amorphous silica with a high degree of purity. SDNs have revealed their indispensable contributions to various disciplines, including medicine, physics, chemistry, biology, and other related domains, owing to their distinct characteristics [27–33]. Based on the varying hydrophilicity of SDNs, they can be classified into two categories: hydrophilic SDNs and hydrophobic SDNs. The majority of SDNs utilised in concrete applications primarily belonged to the hydrophilic category. The primary factor contributing to this phenomenon can be attributed to the effective dispersion of hydrophilic disintegrants in aqueous solutions.

Introduction of SDNs in cement composite materials results in increase in the density of composites, as reported in the literature [34,35]. Increase in the density is due to densification in the microstructure, and this is achieved by formation of more amount of calcium silicate hydrate (CSH) and filling characteristics. Mechanical properties of cementitious materials depend on the amount of CSH present and reduction in the calcium hydroxide content, and enhancement in the mechanical properties is achieved by the addition of substantial proportion of pozzolans [36]. Compared to the control sample, high-performance concrete (HPC) with SDNs and basalt fibre improves the compressive strength and spilt tensile strength about 9.04% and 17.42%, respectively, for 1.2% of SDNs [37]. Increase in the strength characteristics is owing to the increase in CSH and ettringite crystals. Inclusion of SDNs results in the decrease in the concrete pores, improved mechanical properties, and reduction in the diffusion of chloride ions [38,39]. The compressive strength is positively correlated to the load bearing capability and initial stiffness [40]. According to Khanzadi et al. [41], the inclusion of SDNs leads to an increase in the compressive and tensile strengths, particularly during the early stages of hydration. Additionally, improved permeability is observed.

Filling characteristics of pozzolan is achieved using the micro and nano scaled materials like SDNs, which occupies the space between the binder elements [42] and promotes the hydration reaction [38]. Cementitious composites with lesser voids exhibit better properties, and this is achieved by the utilisation of appropriate proportions of components. Presence of SDNs not only fills the voids but also participates in the pozzolanic reaction in high reactivity manner compared to other fillers and pozzolans [43]. Usage of SDNs in cementitious materials is suggested for various applications purpose in the literature [44]. Apart from this, several other nano materials are employed for various purposes in construction sector [45]. For example, usage of nano titanium dioxide can provide self-cleaning and discoloration resistance properties

Table 1
Chemical compositions of OPC.

Components	CaO	SO_3	MgO	Fe_2O_3	SiO_2	Na_2O	K_2O	Al_2O_3	LOI
Percentage (%)	65.25	4.65	1.88	3.98	17.48	0.11	0.39	4.02	2.24

[46,47], and nano carbons are employed for strain sensing in the field of structural health monitoring [48,49]. In addition, usage of carbon nano tubes enhances the ductility of cementitious materials [50,51]. Improved LWFC properties by addition of nano calcium carbonate nanoparticles was reported by Mydin et al. [52].

Apart from the enhancement of the microstructural properties of cementitious composites, SDNs also plays vital role in the stabilisation of hydration products [53]. Hydration of cement results in the primary CSH and free calcium hydroxide, whereas presence of SDNs leads to the pozzolanic reaction (free calcium hydroxide and silicon dioxide from SDN) resulting in the formation of secondary CSH. The secondary CSH has higher density crystal structure compared to other pozzolans [54,55]. These hydration products increase the density of concrete incorporated with SDNs [56] which led to a more tightly packed and denser microstructure, as confirmed by scanning electron microscopy (SEM) [57]. Improvement of the bending strength in the cementitious composites, by incorporation of SDNs results in the rise in its brittleness [58]. Introduction of nano-size SDNs, as supplementary cementitious materials in cementitious system, improves densification in the area of ITZ compared to silica fume [59,60].

Application of SDNs in geopolymer materials derived from high calcium fly ash enhances the microstructural and mechanical properties [61]. Impermeability properties of concrete are improved by addition of SDNs [62]. This is due to the ability of SDNs to occupy the voids in the cementitious system with dual function of acting as an activator and stimulating the pozzolanic reaction at the same time [63]. This leads to the incorporation of SDNs, contributing to the refinement of pore size distribution [64] which substantially decreases the water permeability [65]. It was discovered that the pores have a smaller size and less interconnectivity. Usage of SDNs, as partial replacement of cement, reduces 13.4% of the pore volume [66].

SDNs provide the potential to modify the workability, setting time, consistency, and various other features of concrete [67,68]. Usage of nano SDNs in concrete, results in the fluctuations in the water consumption when more water was added to concrete [69]. A substance possessing a higher level of fineness exhibits an increased surface area, therefore enabling it to absorb a greater quantity of water during the process of mixing. The slump value was decreased upon the introduction of further SDNs into the concrete mixture. The presence of a significant surface area in the SDNs particles, coupled with the presence of unsaturated bonds, results in the migration of water molecules towards the SDNs' surface. This migration leads to the formation of silanol groups [70]. SDNs undergo a fast process of the initial hydration, which intensifies as the surface area of SDNs increases [71]. It has been determined that the maximum allowable proportion of SDNs for achieving an adequate workability is 3% by weight [72,73]. The integration of SDNs reduced the consistency of concrete, leading to an increase in its viscosity [74].

The concrete mixes including nano-silica demonstrated a higher air content compared to the reference mix. The paste containing nanoparticles has an elevated viscosity due to its high specific surface area [75]. Du et al. [76] observed a remarkable improvement in the static and dynamic yield stresses of foamed concrete when a tiny quantity of the SDNs particles was merged. The use of SDNs has the potential to accelerate the hydration time of cement [77,78]. Concrete's long-term durability properties were investigated by Quercia et al. [79] by using 3.8% of SDNs. Du and Pang [80] observed that the utilisation of colloidal SDNs at a concentration range of 1.5–2.0% resulted in the optimal mechanical properties and durability.

Considering all these factors, conducting a study on the use of SDNs in the cementitious materials such as ultra-lightweight foamed concrete (ULFC) still needed further exploration. This study would have a significant impact on both sustainability and enhancement of mechanical properties. Previous research has examined various factors related to the incorporation of SDNs into ULFC in varying proportions. Consequently, the microstructural enhancements have exhibited advantages in both tensile and compressive strengths, as well as durability attributes. Thus far, there has been a lack of research performed on the integration of SDNs in the context of ULFC. This study assesses the fresh, mechanical, microstructural, and thermal properties of ULFC with varying weight percentages of SDNs.

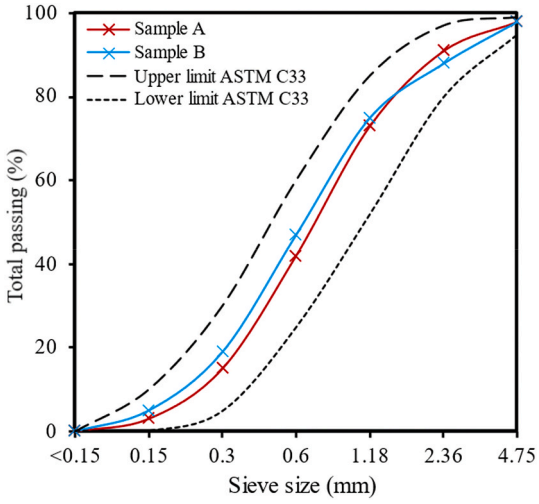

Fig. 1. Sieve analysis curve for fine sand.

1.1. Research gap and novelty of study

Currently, there is a lack of study on the impact of SDNs on the properties of ULFC, both in its fresh and hardened states. While the options for commercially accessible SDNs in ULFC are limited, they are highly promising for this particular application. Research has been done on incorporating SDNs into LWFC, as already reported in the literature, but there is still room for exploration in the area of SDNs for the development of ULFC. The mechanical properties of ULFC are evaluated to understand the effects of SDNs. There are still numerous ambiguities around the process through which SDNs can potentially alter the properties of ULFC, which are investigated in the current research. The lack of clarity on this issue must be resolved. Therefore, it is crucial for assessing the impact of SDNs alteration on the properties of ULFC. The contribution of improved mechanical qualities is confirmed through morphological investigation utilising SEM and mercury intrusion porosimetry (MIP).

Table 2
Protein foaming agent properties.

Components	Properties
Density (kg/l)	1.125
Specific gravity	1.05
Acidity (pH)	6.33
Colour	Light brown
Boiling point (°C)	140
Expansion fraction	22 ×
Viscosity (cps)	595

Table 3
Physical properties of OPC, sand, and SDNs.

Properties	OPC	Sand	SDNs
Specific gravity	3.14	2.53	2.18
Density (kg/m^3)	1460	1760	1995
Fineness modulus	–	2.35	2.21
Moisture absorption (%)	2.89	2.20	0.48
Bulk porosity (%)	–	27	25

2. Experimental program

2.1. Materials

ULFC mixes were produced using ordinary Portland cement (OPC) Type CEM-1, fine sand, SDNs, potable water, and a foaming agent. OPC with a grade 525 MPa was supplied by cement industries of Malaysia Berhad, meeting the specifications given in MS522 [81]. Table 1 presents an overview of the chemical constituents of OPC. Fine sand was acquired from a local provider, possessing a specific gravity value of 3.15. Fine sand followed a process of sifting to separate particles that were capable of passing through a sieve with a mesh size of 4.75 mm. To mitigate the occurrence of harmful microbes, the sand underwent a process of thermal treatment at a temperature of 105 °C for a duration of 48 h. Fig. 1 depicts the examination of particle size for fine sand utilised in the present investigation, adhering to ASTM C33-03 [82]. The water used to produce ULFC mixes consisted of potable tap water that met the specifications mentioned in BS EN 3148 [83]. Subsequently, the selection of the foaming agent utilised for the creation of a durable foam was derived from a surfactant obtained from proteins, aligning with the specifications outlined in ASTM C796M – 19 [84]. The proteinaceous foaming agent was combined with water in a proportion of 1:20 and underwent aeration until it reached a density of 70–75 kg/m^3. Table 2 lists the characteristics of the foaming agent employed in the generation of a durable foam. SDNs were acquired from Biotek Abadi Sdn. Bhd., Malaysia. Table 3 summarises the physical parameters of OPC, sand, and SDNs. SDNs exhibit a purity level of 99.9%. Fig. 2(a) illustrates the transmission electron microscopy (TEM) of SDNs. The TEM study revealed a diameter range between 20 and 40 nm. Regarding the crystalline structure of SDNs, the XRD result shown in Fig. 2(b) indicates a distinct and wide peak detected at a 2θ angle of 23°. This observation implies that the particles of SDNs displayed an amorphous form.

Table 4
Optimised proportions of SDNs in cementitious system.

Reference	Type of mix	SDNs percentage (%)	Size of SDNs (nm)
Shaikh et al. [85]	Concrete	2.00	25
Sobolev et al. [86]	Concrete	2.00	5–50
Singh et al. [87]	Cement paste	5.00	40–50
Berra et al. [88]	Cement paste	3.80	10
Qing et al. [89]	Cement paste	5.00	–
Mukherjee et al. [90]	Cement mortar	3.00	8–20
Qian et al. [91]	Cement mortar	2.25	10
Heikal et al. [92]	Cement mortar	2.00	15

Table 5
Mix design of ULFC.

Mix code	Density (kg/m^3)	SDNs (%)	SDNs (kg/m^3)	OPC (kg/m^3)	Sand (kg/m^3)	Water (kg/m^3)	Foam (kg/m^3)
ULFC-0.0	400	0.0	0.00	155.4	233.1	77.7	49.4
ULFC-0.5	400	0.5	2.33	155.4	233.1	77.7	49.4
ULFC-1.0	400	1.0	4.66	155.4	233.1	77.7	49.4
ULFC-1.5	400	1.5	6.99	155.4	233.1	77.7	49.4
ULFC-2.0	400	2.0	9.32	155.4	233.1	77.7	49.4
ULFC-2.5	400	2.5	11.65	155.4	233.1	77.7	49.4

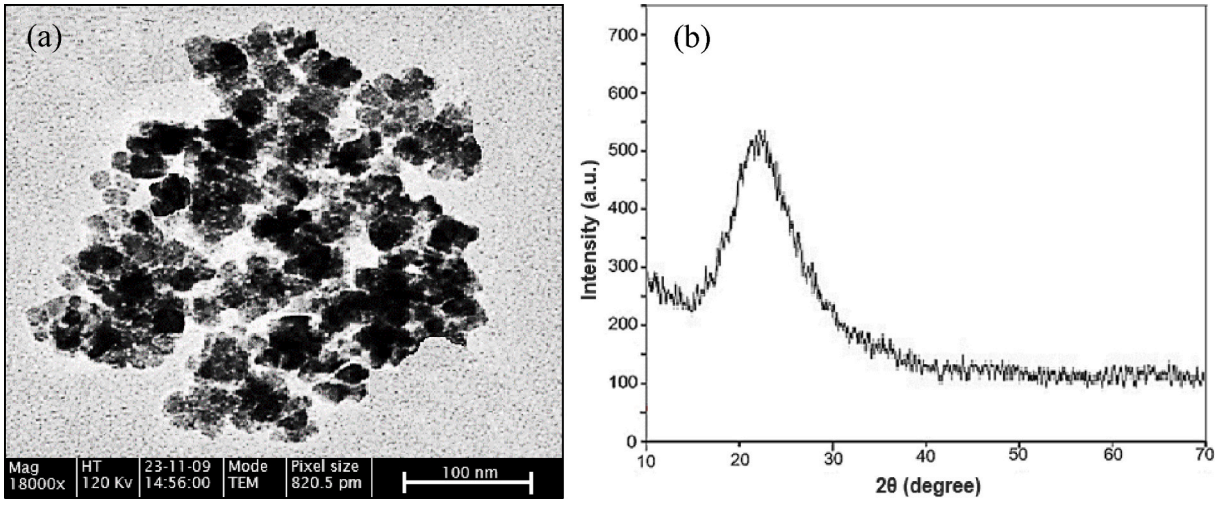

Fig. 2. (a) TEM of SDNs, (b) XRD pattern of SDNs.

Fig. 3. Manufacturing process of ULFC.

2.2. Mix proportions

ULFC with a low density of 400 kg/m^3 was produced by varying the amounts of SDNs. The water-to-cement ratio was established at 0.5, while the ratio of cement to sand was constantly maintained at 1:1.5. To examine the impact of adding SDNs on the different properties of ULFC, various proportions of SDNs were considered. These proportions included 0.0% (served as a control), 0.5%, 1.0%, 1.5%, 2.0%, and 2.5% based on the weight fraction of the ULFC mixture. The selection of the SDN proportions ranged from 0.0% to 2.5% based on a review of the existing research undertaken by various scholars on cementitious systems, as mentioned in Table 4. As far as the optimal proportion of SDNs is concerned, there is clearly a state of ambiguity. Table 5 presents the mix design of ULFC. A total of 6 mixes were prepared and tested.

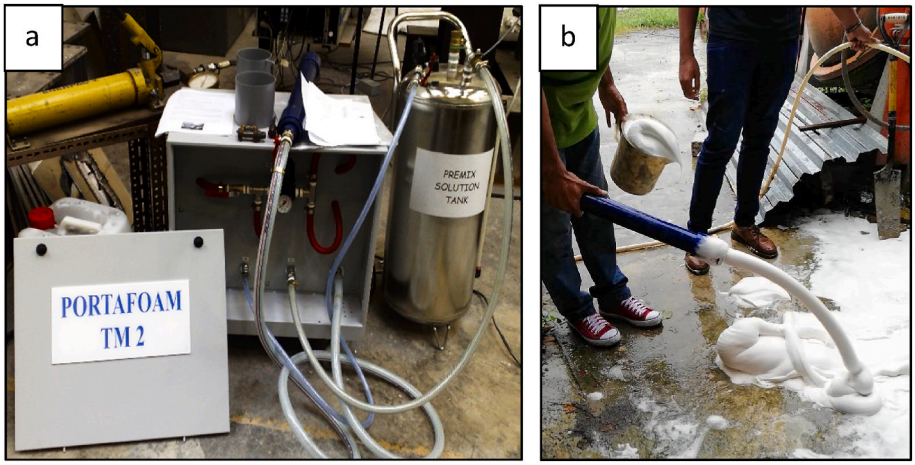

Fig. 4. Preparation of prefabricated foam: (a) Porta foam TM-2 generator runs from an air compressor, (b) production of stable prefabricated foam.

2.3. Manufacturing process of ULFC

The production process of ULFC has several essential stages, including mixing, sample casting, and curing phase. The control ULFC samples were produced using a mixture of fine sand, OPC, potable water, and stable protein-based foam. Fig. 3 demonstrates the various steps involved in ULFC manufacturing. Initially, a combination of OPC, sand, and SDNs was dry mix utilising a drum mixer for approximately 3 min. Then, the dry mix was thoroughly blended by gradually adding water, resulting in a homogeneous mixture after 4 min of mixing. Prior to introducing the premade foam into mortar slurry, a comprehensive assessment was carried out on mortar. This was done to evaluate its density and workability.

The foam generator employed in this study was Porta foam TM-2 model powered by an air compressor and comprises of a holding tank, foaming unit, and discharge unit, as depicted in Fig. 4(a). The primary function of the holding tank is to contain the diluted protein-based foaming agent. The foaming agent was mixed with water in a ratio of 1:22 and later transmitted via a foaming unit and discharge unit resulting in the production of prefabricated foam, as shown in Fig. 4(b). The foam density was carefully tested and regulated to a value of 70–75 kg/m^3 prior to its introduction into the mixer drum. After the foam has been introduced into the mixer, it was imperative to continue the mixing process until bubbles were absent. To attain a specified ULFC density, it was necessary to measure the weight of 1 L of the mixture until it met the targeted density. Subsequently, the ULFC fresh mix was introduced into the steel moulds. Demoulding for all samples was conducted 24 h following production. Afterwards, all specimens were treated to a curing process and tested at various ages.

2.4. Testing of specimens

This section outlines the testing methodologies employed to assess the properties of ULFC incorporating different proportions of SDNs. The parameters under investigation include the fresh state characteristics, transport properties, mechanical performances, thermal properties, and microstructural characteristics.

2.4.1. Fresh state properties

A flow table test was done to evaluate the flowability of ULFC mixtures in accordance with ASTM C230-97 [93]. In addition, the initial and final setting times of ULFC were determined according to the guidelines of BS EN 196-3 [94]. Following the guidelines provided in BS 12350-6 [95], different ULFC mixture densities were also identified throughout the mixing process.

2.4.2. Transport properties

The measurement of the porosity provides a quantitative assessment of the volumetric magnitude of voids present inside ULFC. The porosity test was conducted utilising the vacuum saturation apparatus. The test for the water absorption was then performed following the guidelines outlined in BS EN 1881-122 [96]. The test was completed on the 7th, 14th, 28th, and 90th days using cylindrical specimens measuring 75⌀ × 100 mm. Then, the sorptivity test was carried out using the recommended methodologies delineated in ASTM C1403-15 [97]. The sorptivity test was executed on the 7th and 28th days with a cube specimen of 50 × 50 × 50 cm. Subsequently, the assessment of the intrinsic air permeability was done following the methods put forth by Cabrera and Lynsdale [98]. The apparatus was used to quantify the volumetric flow rate of air passing through the ULFC specimens. The experiment encompassed ULFC cylinders measuring 45⌀ × 50 mm in dimensions. The study employed the rapid chloride permeability test to assess the ULFC's resistance to the chloride ion penetration, following the guidelines outlined in ASTM 1202-19 [99]. The experiment was performed utilising a prism ULFC sample, which had a thickness of 50 mm and a diameter of 100 mm. The experiment was done on day 28 and day 90.

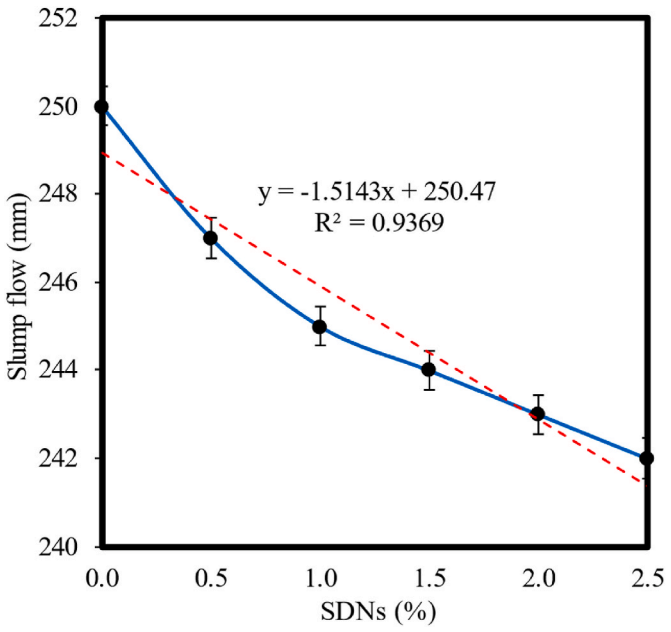

Fig. 5. Slump flow of ULFC mixes containing different percentages of SDNs.

2.4.3. Thermal properties

A hot plate with guided heat conduction was used to assess the thermal properties of the ULFC samples, including the thermal conductivity, specific heat capacity, and thermal diffusivity. The technique is in accordance with ASTM C177-19 [100]. The ULFC samples being tested are 20 × 20 × 8 mm in size. It consisted of a sensor sandwiched between two composite discs, followed by another two discs.

2.4.4. Mechanical properties

A prism with dimensions of 100 × 100 × 500 mm was employed in the flexural test. The testing procedures were conducted in accordance with BS EN 12390-5 [101]. Next, a split tensile test was done as per the prescribed guidelines in BS EN 12390-6 [102]. Cylindrical specimens of 100⌀ × 200 mm in diameter were subjected to testing. In addition, a series of compression tests were conducted using cubes measuring 100 × 100 × 100 mm, following the guidelines provided in BS12390-3 [103]. Experiments were carried out to evaluate the flexural, split tensile, and compression properties of the specimens at different curing durations of 7, 14, 28, 56, and 90 days. The modulus of elasticity of the ULFC specimens was determined by employing a 28-day curing period following ASTM C469 [104].

2.4.5. Microstructural properties

The pore size distribution in ULFC was assessed using the MIP technique, based on the guidelines specified in ASTM D4404-18 [105]. In addition, the ULFC specimens were subjected to the SEM analysis at a magnification of 120 × after the 28-day curing time, as per the specifications outlined in ISO 16700 [106]. Specimens measuring 10 × 10 × 10 mm were fabricated from every batch for the analysis.

3. Results and discussion

3.1. Fresh state properties

3.1.1. Workability

ULFC with excellent quality has a satisfactory workability (around 250 mm spread diameter) in fresh condition and develops adequate strength. Generally, the larger the measured spread diameter, the better the workability, indicating that ULFC flows easily while also remaining free of segregation. In Fig. 5, slump flows are illustrated for the ULFC

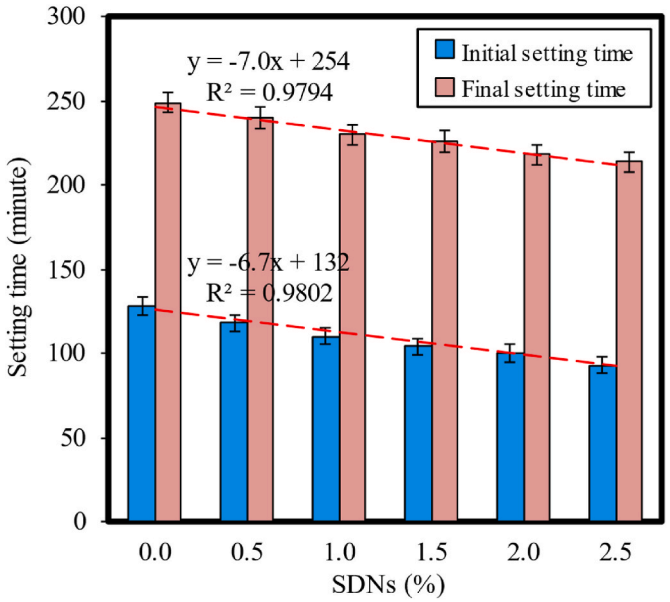

Fig. 6. Initial and final setting times of ULFC containing different percentages of SDNs.

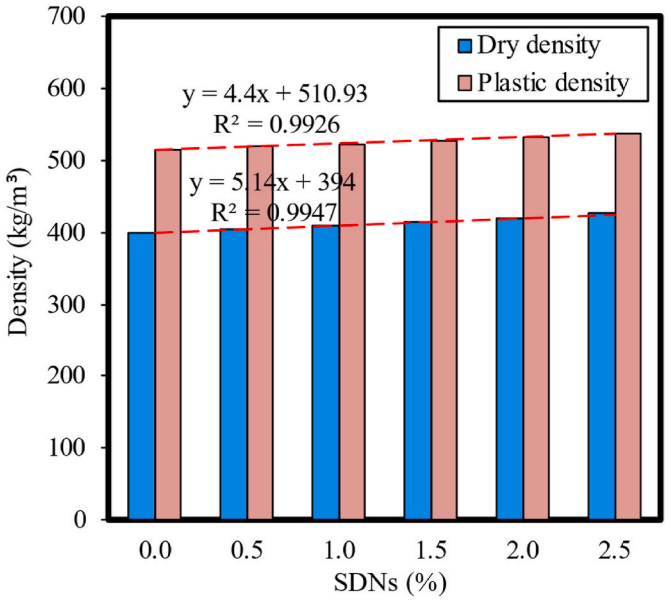

Fig. 7. Plastic and dry densities of ULFC containing different percentages of SDNs.

mixtures with different proportions of SDNs. The slump flow of the ULFC mixtures with the addition of 0.5%, 1.0%, 1.5%, 2.0%, and 2.5% of SDNs was measured and compared to those of the control mix. Compared to the control ULFC mixture, all the studied SDNs blended ULFC mixtures displayed lower slump values. A slump flow of 250 mm was recorded for the control ULFC mix. Adding 0.5%, 1.0%, 1.5%, 2.0%, and 2.5% of SDNs resulted in a 1.2%, 2.0%, 2.4%, 2.8%, and 3.2% reduction in the slump flow, respectively. Thus, the ULFC mixtures with the increased SDN content indicated a correlation with a reduction in the slump flow value. In this study, SDNs were found to have a higher level of the water absorption than other materials, leading to greater water consumption and decreased flowability [107].

Moreover, the decrease in the slump flow with the addition of SDNs may be explained by the increase in the surface area after the addition of SDNs, which requires more water to wet the cement particles. SDNs have a higher specific surface area, and therefore demand more water, which can have an impact on the slump flow in the ULFC mixtures. Further, when the proportion of fine nanoparticles in cementitious composites of ULFC is increased, the rheological properties of pastes will be affected, resulting in changes in the workability of ULFC fresh mixtures [108]. In addition, the presence of unsaturated bonds in SDNs renders them exceptionally reactive, leading to the attraction of water molecules towards their surfaces. The interaction between water and SDNs particles causes the formation of silanol groups (Si–OH), which subsequently reduces the amount of free water present in the mixture [109]. The findings presented in this study are consistent with the results reported in prior studies on SDNs concrete [66,68]. Nevertheless, the observed decrease in the slump flow, attributed to the incorporation of SDNs up to 2.5%, was rather insignificant. Furthermore, even with this reduction, the minimum slump value recorded in the mixture was 242 mm, which is still regarded exceptionally high in the context of ULFC. An evident relationship was found between the percentage increase of SDNs and the reduction in the workability of ULFC, with a correlation coefficient of 0.9369. As the proportion of SDNs in ULFC increases, there is a greater reduction in the workability of the mix.

3.1.2. Setting time

Fig. 6 elucidates the initial and final setting times of ULFC containing different percentages of SDNs. The initial and final setting times of the ULFC mixtures containing 0.5%, 1.0%, 1.5%, 2.0%, and 2.5% of SDNs were determined and contrasted to those of the control mixture. When compared to the control ULFC mixture, all the ULFC mixtures incorporated with SDNs exhibited shorter initial and final setting times. The initial and final setting times for the control ULFC mixture were recorded as 128 and 251 min. Adding 0.5%, 1.0%, 1.5%, 2.0%, and 2.5% of SDNs, the initial and final setting times reduced by 7.81%, 14.06%, 18.75%, 21.88%, and 27.34% and by 3.61%, 7.63%, 9.24%, 12.45%, and 14.06%, respectively. The increased SDN content in the ULFC mixtures decreased the initial and ultimate setting times. The reduction in the setting times seen in ULFC with an increased proportion of SDNs suggests that SDNs demonstrates a faster hydration reaction rate compared to cement. This can be attributed to the distinctive surface effects, micron-sized particles, and greater surface energy exhibited by SDNs [38].

Reduced particle sizes facilitate a prompt augmentation in the surface area, resulting in an accelerated proliferation of surface atoms. The surface atoms display an elevated degree of reactivity and instability, leading to an intensified rate of reaction. Therefore, it is important to use a prudent strategy when determining the duration for which paste is allowed to set in the context of SDNs [64]. The significant decrease in the setting time of the ULFC mixture including 2.5% of SDNs can be ascribed to the accelerated growth of the CSH gel. This phenomenon leads to the production of a more viscous ULFC mixture, resulting in the reduced initial and final setting times. An explicit relationship was noted between the percentage increase in SDNs and the reduction in both the initial and final setting times, supported by correlation coefficients of 0.9082 and 0.9794, respectively. As the rate of the SDNs addition increases, there is a corresponding decrease in both the initial and final setting times.

3.1.3. Density

Fig. 7 depicts the plastic and dry densities of ULFC including varying proportions of SDNs. The plastic and dry densities of ULFC mixtures, which included varying percentages of 0.5%, 1.0%, 1.5%, 2.0%, and 2.5% of SDNs, were measured and compared to the densities of the control mixture. In comparison to the control ULFC mixture, all the ULFC mixtures that were integrated with SDNs displayed increased values of plastic and dry densities. When adding 0.5%, 1.0%, 1.5%, 2.0%, and 2.5% of SDNs, the plastic density and wet density increased by 0.78%, 1.36%, 2.33%, 3.29%, and 4.26%, and by 1.25%, 2.25%,

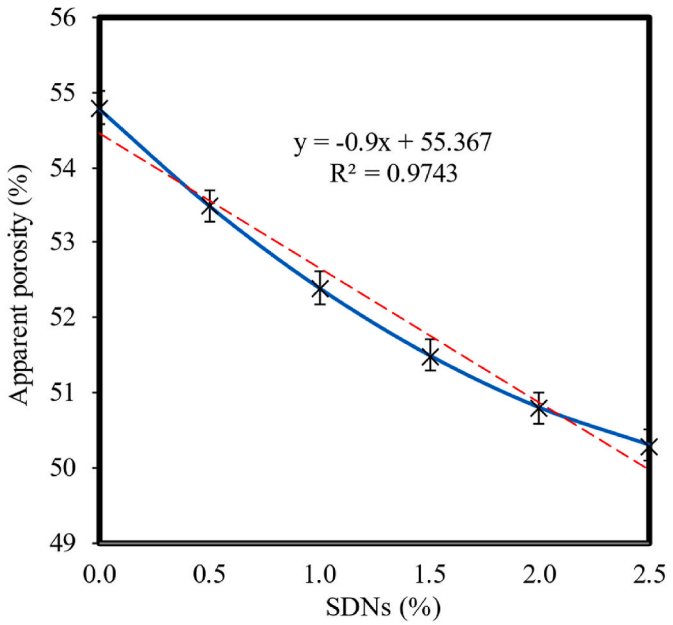

Fig. 8. Apparent porosity of ULFC containing different percentages of SDNs.

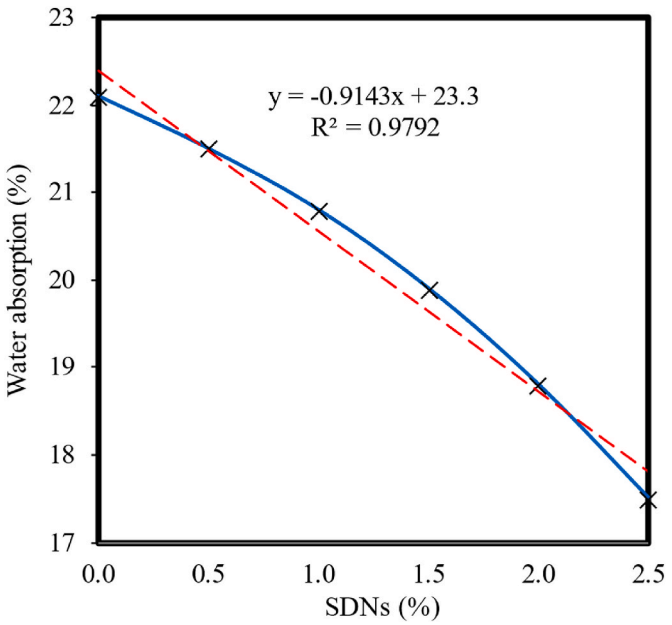

Fig. 9. Water absorption of ULFC containing different percentages of SDNs.

3.50%, 5.00%, and 6.50%, respectively. The observed increase in the plastic and dry densities of ULFC in the presence of SDNs might be attributed to the comparatively larger bulk density of SDNs when compared to fine sand, as presented in Table 3. The presence of SDNs in the ULFC mix increases its overall density due to the fact that light particles have a lower density than SDNs [110]. Consequently, the inclusion of SDNs leads to higher plastic and dry densities. A direct correlation was witnessed between the percentage addition of SDNs and the plastic and dry densities, with correlation coefficient (R^2) values of 0.9926 and 0.9947, respectively. The higher the addition rate of SDNs, the greater the increase in the plastic and dry densities of the ULFC mixes.

3.2. Transport properties

3.2.1. Apparent porosity

The enhancement of microstructure characteristics in cement-based materials through the reduction of the porosity and improvement of pore arrangement is a generally acknowledged outcome of the pozzolanic and filler effects caused by the presence of SDNs. Fig. 8 illustrates the observed porosity of the ULFC specimens including varying proportions of SDNs. The evidence shown in Fig. 8 indicates a noticeable reduction in the apparent porosity of the ULFC mixtures with the incorporation of SDNs. The addition of SDNs resulted in a decrease in apparent porosity by 2.37%, 4.38%, 6.02%, 7.30%, and 8.21% when the SDN concentrations were 0.5%, 1.0%, 1.5%, 2.0%, and 2.5%, respectively. The addition of SDNs to the ULFC base mix leads to a significant crystallization nucleation effect. This can be attributed to the high energy demonstrated by SDNs, which results in the absorption of a substantial amount of the hydration product. Consequently, structure of the CSH gel is formed. Moreover, the initial reaction of pozzolan occurs at the silica surface, forming a robust CSH gel. This gel subsequently generates greater CSH gels, which effectively occupy the small pores inside the specimen, contributing to the enhancement of the pore structure. SDNs can be regarded as evolving nanoscale substance that possess the potential to greatly enhance the pore structure of materials based on cementitious compositions. Wang et al. [111] discovered that the incorporation of 2.5% of SDNs in concrete resulted in a reduction of roughly 6% in the porosity. Based on the findings of Said et al. [112], the inclusion of 6% of SDNs led to a significant reduction of critical voids by up to 40% and a corresponding increase in the proportion of micro-pores by 4%. The primary cause of this phenomenon can be predominantly ascribed to the pozzolanic, and filler effects exhibited by the particles of SDNs. They reached the conclusion that there was a considerable decrease in both the overall porosity and the critical pore size as the amount of SDNs increased. In addition, Oltulu and Sahin [113] performed a study that evaluated the pore structures of mortar by using silica fume at varying proportions of SDNs, precisely 0.50%, 1.25%, and 2.50%. The findings of the study indicated that the inclusion of 0.5% and 1.25% of SDNs in mortar resulted in a significant decrease in the volume of pores and total porosity compared to the control sample, with reductions of 45% and 48%, respectively. Singh et al. [3] studied the porosity of concrete in the presence of 9% of SDNs. The researchers made the observation that the addition of SDNs reduced the porosity in CSH from 28% to 11%, while simultaneously increasing the porosity of the gel from 13% to 21%, in comparison to the control mixture. The results of their study revealed that the incorporation of SDNs has the potential to reduce the presence of uncertain pores, despite the increase in fewer harmful pores. A clear linear relationship was seen between the percentage rise in SDNs and the decrease in apparent porosity, as evidenced by a correlation coefficient of 0.9743. As the amount of incorporating SDN increases, there is a simultaneous drop in the apparent porosity readings of ULFC.

3.2.2. Water absorption

The water absorption capacity of ULFC can be influenced by its open porosity and homogeneity. The durability of ULFC may be affected owing to its excessive water absorption level, as this allows for the penetration of harmful solutes and ions into the inside of the material via its pores in the presence of water. The results obtained for ULFC water absorption containing different percentages of SDNs are displayed in Fig. 9. The addition of SDNs was found to be effective in reducing the water absorption of the ULFC specimens. It can be seen that the amount of absorbed water in the samples decreased by increasing SDNs. The addition of SDNs by 0.5%, 1.0%, 1.5%, 2.0%, and 2.5% decreased the water absorption in the samples by 2.71%, 5.88%, 9.95%, 14.93%, and 20.81%, respectively. The findings of this study were in-line with the previous research. According to Jalal et al. [68], the incorporation of 2% of SDNs decreased the water absorption capacity of concrete by 58% in comparison to the control mix. Furthermore, they observed that the

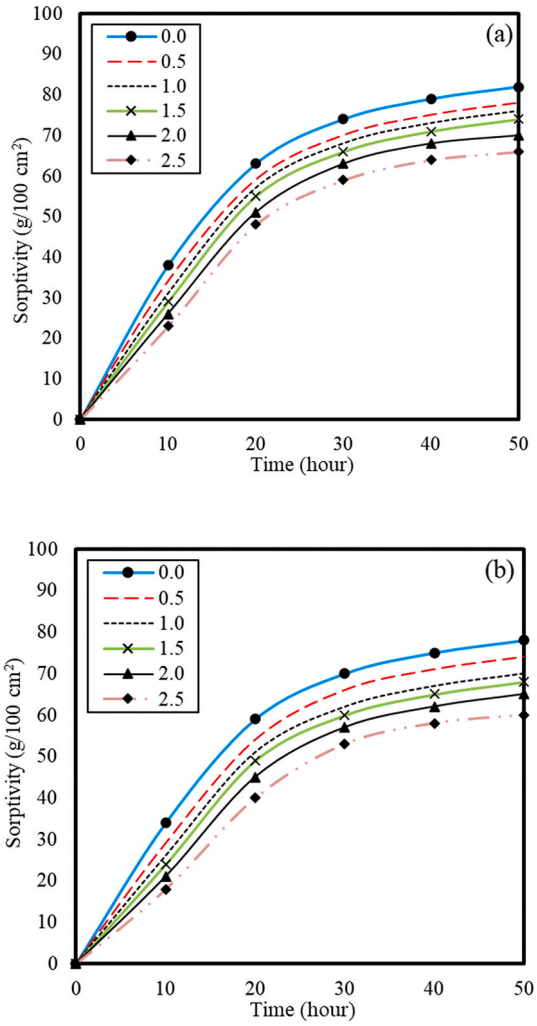

Fig. 10. Sorptivity of ULFC containing different percentages of SDNs: (a) 7-day, (b) 28-day.

depth of absorbed water would decrease more notably at longer times of the test. The stiffening of the internal structure of ULFC, resulting from the generation of CSH during the hydration process, leads to the filling of pores within ULFC and consequently reduces its water absorption capacity [114].

Chithra et al. [116] reported that small substations of cement by 2% of SDNs led to a reduction of the water absorption. The efficiency of very fine SDNs particles, which block the pores and improve the microstructure of the specimens, is another reason for the reduction of the water absorption values. The progress of the pozzolanic reactions of SDNs leads to the rupture of interconnected pores and the reduction of total pore volume, thereby inhibiting the improvement of the water absorption capacity of cement-based materials [117]. Tobón et al. [118] used SDNs as cement replacement in concrete. They found that the water absorption of concrete replaced by 5% and 10% of cement reduced dramatically. They concluded that high specific surface area and well-dispersion of SDNs can be considered for their power in the acceleration of the pozzolanic reactions. The findings showed a substantial positive correlation with an R^2 value of 0.9792 between the increase in SDNs and the decrease in the water absorption capacity. As the percentage of SDNs increases, there is a corresponding decrease in the water absorption values of ULFC.

3.2.3. Sorptivity

Sorptivity is a significant parameter that serves as an indicator for assessing the transport properties of porous cementitious materials. It

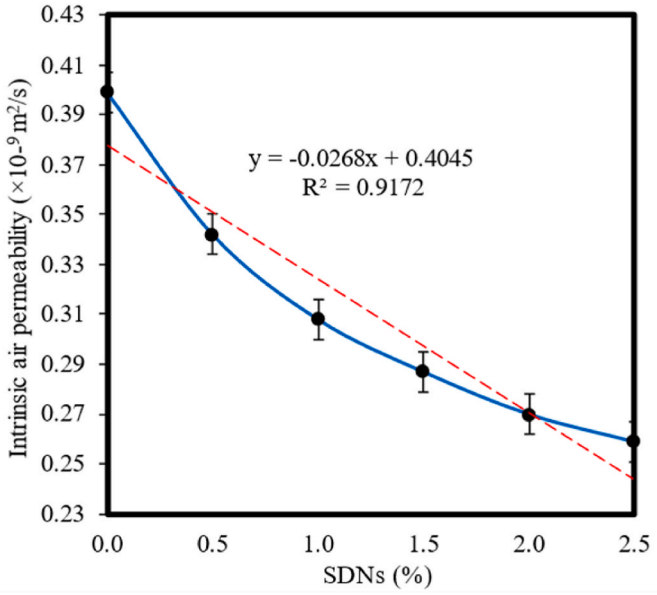

Fig. 11. Intrinsic air permeability of ULFC containing different percentages of SDNs.

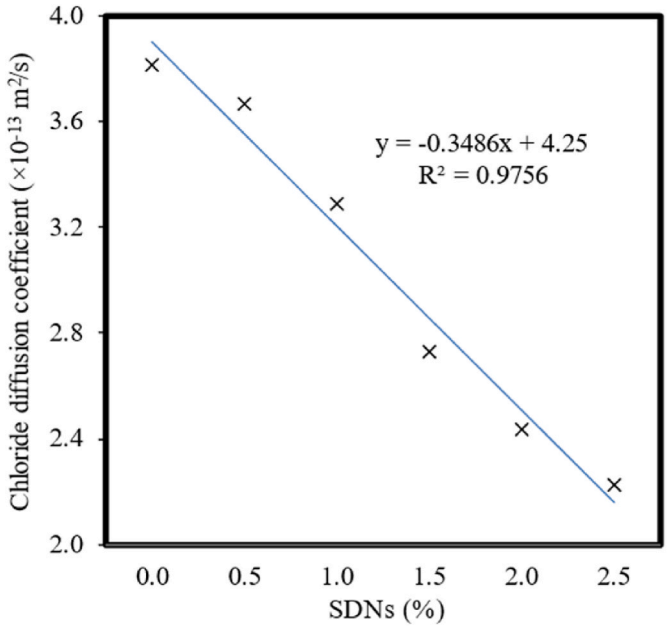

Fig. 12. Chloride diffusion coefficient of ULFC containing different percentages of SDNs.

effectively characterises the absorption and transport characteristics of water via capillary passages inside these substances. Sorptivity of the ULFC mixes with varying percentages of SDNs at different ages are illustrated in Fig. 10(a and b). Results depict that integration of SDNs in the ULFC base mixes decreased the capillary network for all the SDNs percentages. After 50 h and at 28 days of curing, the addition of SDNs by 0.5%, 1.0%, 1.5%, 2.0%, and 2.5% decreased the sorptivity in the samples by 5.13%, 10.26%, 12.82%, 16.67%, and 23.08%, respectively. The primary pathway for water migration in cement-based materials is widely recognised to be through the capillary pores. According to Abd Elrahman et al. [115], the inclusion of SDNs facilitates the consolidation of the microstructure and diminishes the porosity of ULFC, particularly the interconnectivity of pores. The results proved that the refinement of the pore structure of ULFC with the presence of SDNs was a key factor that improved the characteristics of the ULFC samples. In fact, most aspects of the durability of ULFC are directly related to its porous structure, since capillary pores are responsible for the fluids' migration in the ULFC cementitious matrix [21]. Therefore, as the value of the sorptivity decreases, the resistance to aggressive environments enhances significantly. When water penetrates the interior of ULFC, it encounters much smaller pores, such as the gel pores, which explains the lower sorptivity with the presence of SDNs. Moreover, plenty of the gel pores were present in the transition zone between the fine aggregate and its interface. When water penetrates the pores, it would form the stable or unstable form of water and air, which would reduce the sorptivity values

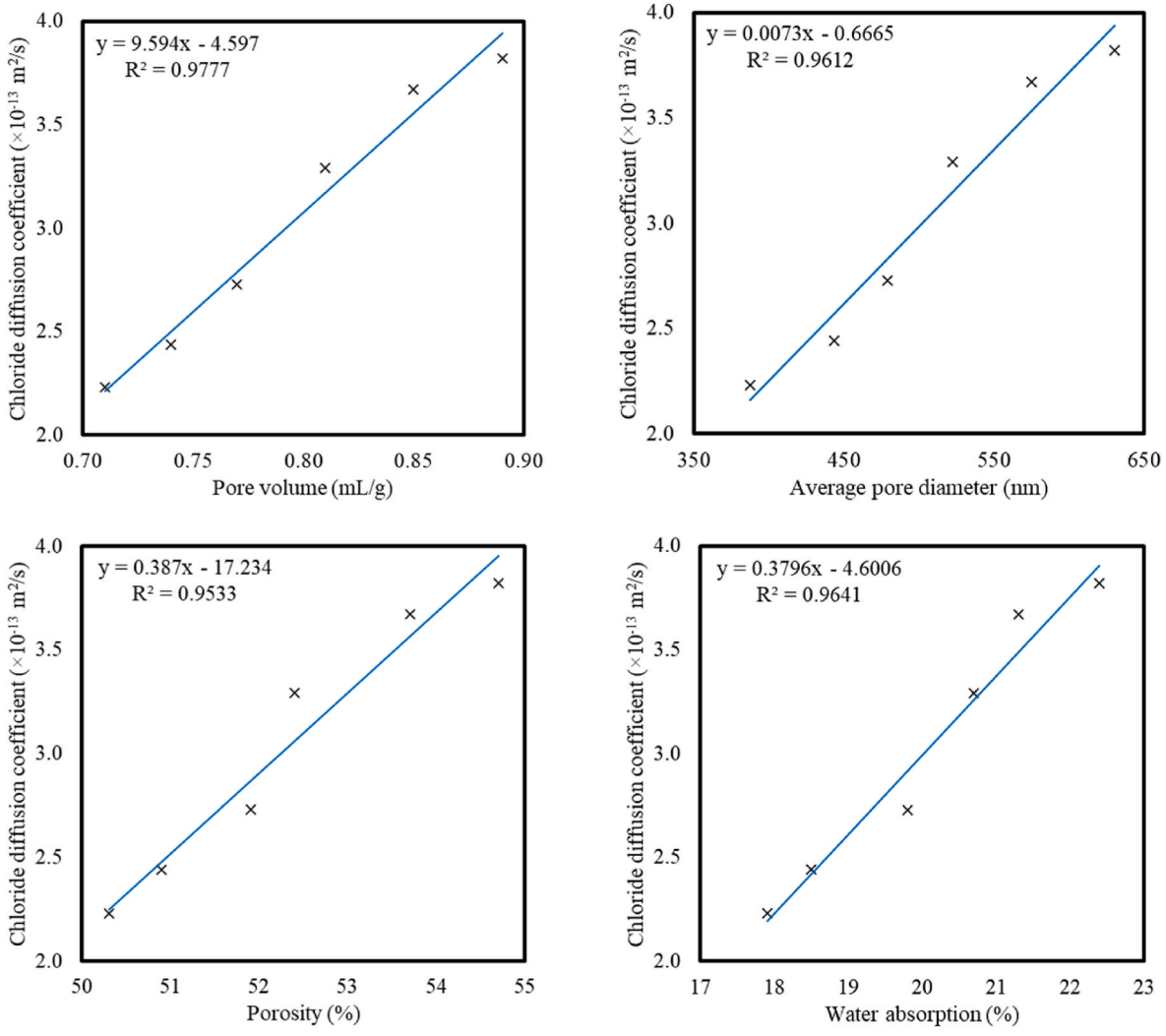

Fig. 13. Correlation between chloride diffusion coefficient and pore structure parameters of ULFC.

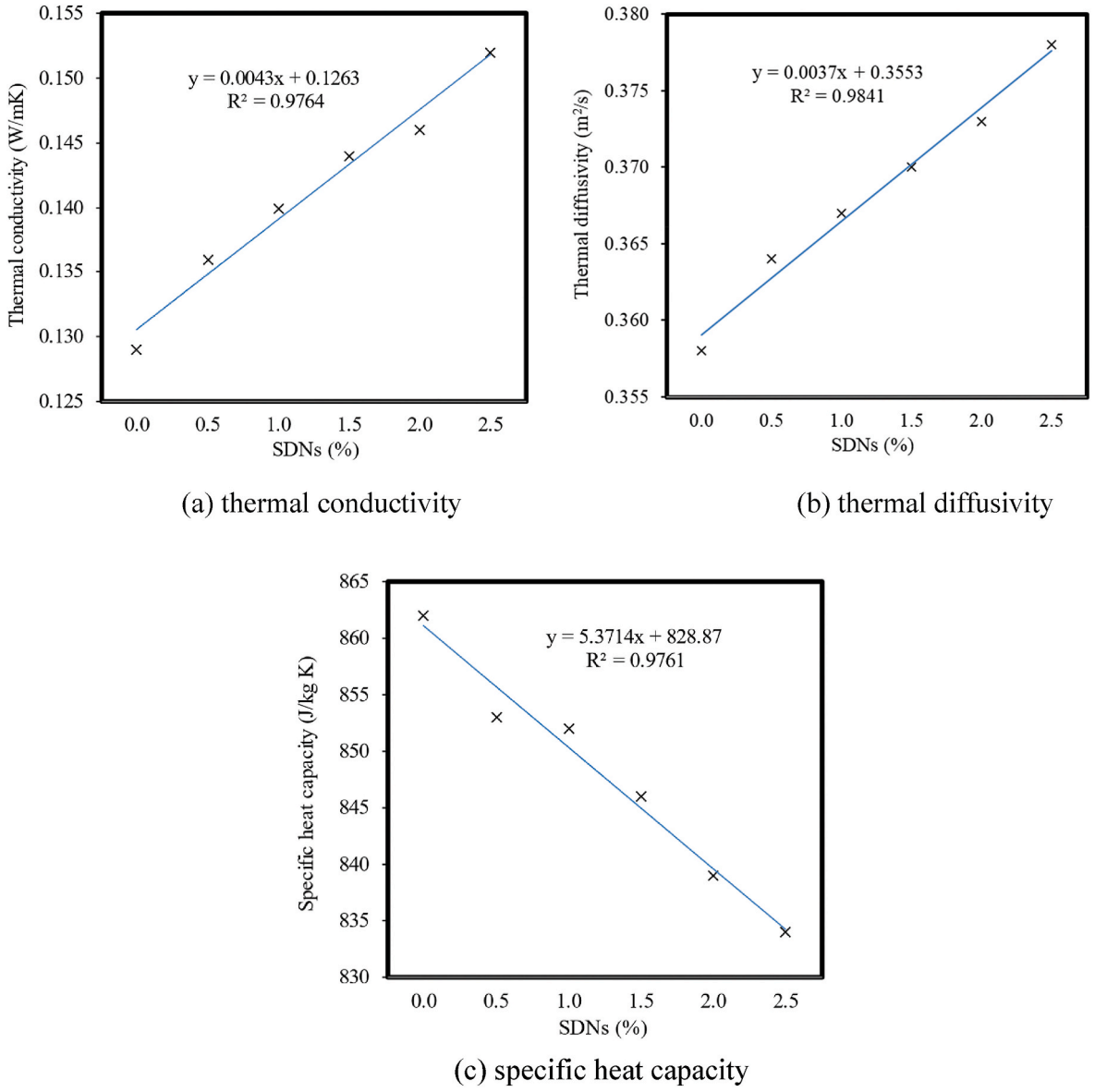

Fig. 14. Thermal properties' parameters of ULFC containing varying percentages of SDNs.

[51].

3.2.4. Intrinsic air permeability

Fig. 11 presents the intrinsic air permeability of ULFC containing different percentages of SDNs. The intrinsic air permeability of ULFC mixtures containing 0.5%, 1.0%, 1.5%, 2.0%, and 2.5% of SDNs were determined and contrasted to those of the control mixture. When compared to the control ULFC mixture, all the ULFC mixtures incorporated with SDNs exhibited lower intrinsic air permeability values. The intrinsic air permeability for the control ULFC mixture was recorded as 0.399×10^{-9} m^2/s. Adding 0.5%, 1.0%, 1.5%, 2.0%, and 2.5% of SDNs, the intrinsic air permeability reduced by 14.29%, 22.81%, 28.07%, 32.33%, and 35.09%, respectively. This implies that SDNs function as an accelerator for the process of the cement hydration, while also serving as a substance that enhances the internal microstructure of ULFC. Consequently, the microstructure of ULFC exhibited the improved uniformity and reduced porosity due to the incorporation of SDNs [120]. When the ULFC mixture consists of a relatively high proportions of SDNs, the adhesion properties of the mixture are enhanced, whilst the internal porosity of ULFC is reduced [121]. Consequently, there is a reduction in the gas permeability. The enhanced filler effect of SDNs can be attributed to the incorporation of nano-sized fine particles. Additionally, the high pozzolanic activity of SDNs remarkably augments the formation of the CSH gel. The enhancement of the microstructure inside ITZ has the potential to boost the composition of the CSH gel, leading to a significant reduction in the intrinsic air permeability. These reactions lead to an increase in the homogeneity and strength of ITZ, as well as a decrease in their diameter. This results in a reduced probability of micro cracks and a more uniform distribution of particles, which ultimately contributes to the refinement of the grain structure in the hydrated cement paste within ITZ [122]. Therefore, the incorporation of SDNs into cement has the potential to lead to the reorganization and enhancement of the physical and chemical microstructures of ULFC. A strong positive association was seen between the percentage increase in SDNs and the reduction in the intrinsic air permeability of the ULFC mixes, as indicated by an R^2 value of 0.9172. As the percentage of SDN grows, there is a corresponding decrease in the intrinsic air permeability.

3.2.5. Chloride diffusion coefficient

Fig. 12 displays the chloride diffusion coefficient of ULFC

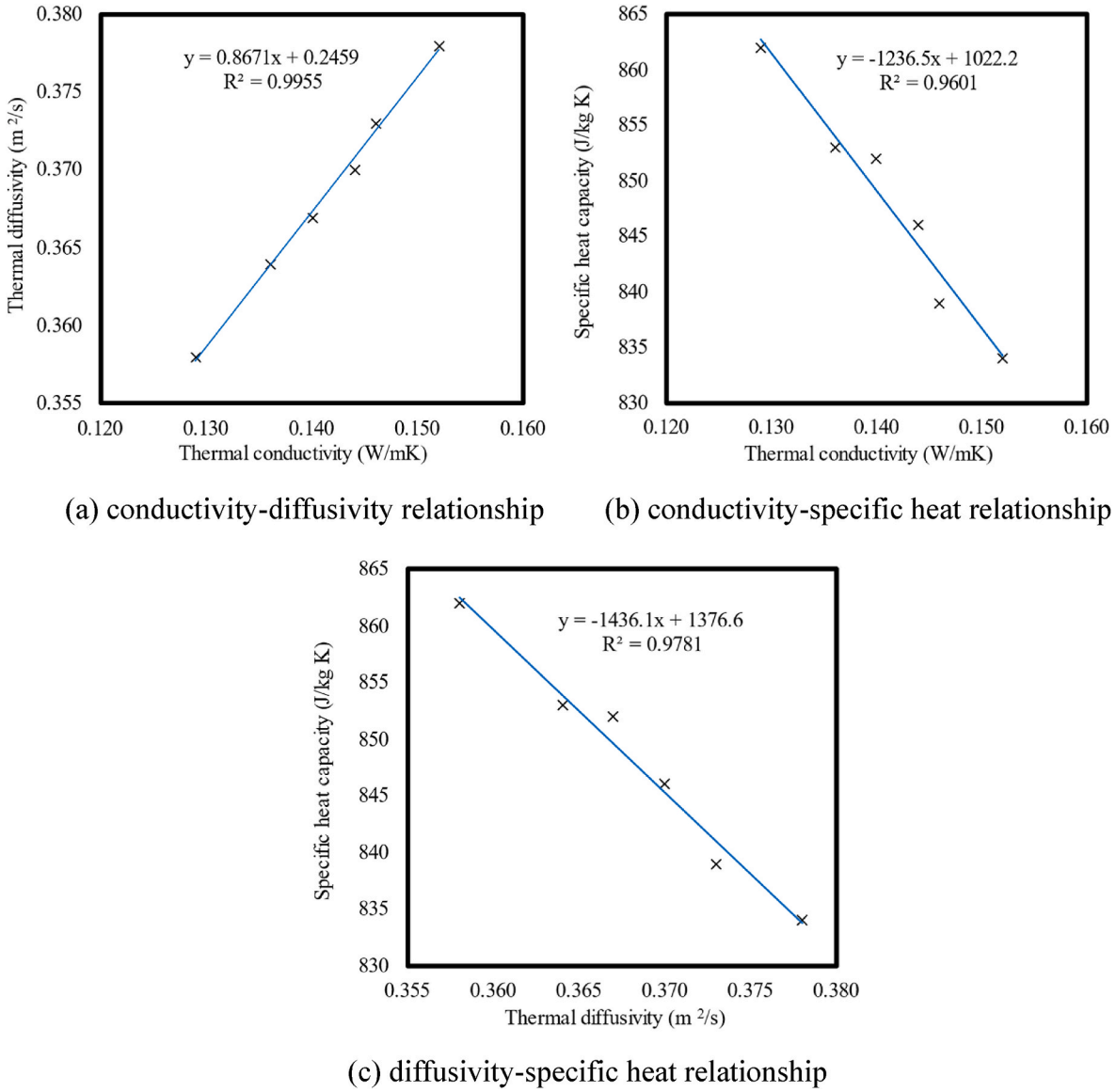

Fig. 15. Correlation between thermal properties' parameters of ULFC containing varying percentages of SDNs.

incorporating varying proportions of SDNs. The chloride diffusion coefficient of the ULFC mixtures with varying percentages of SDNs at 0.5%, 1.0%, 1.5%, 2.0%, and 2.5% were measured and compared to the chloride diffusion coefficient of the control mixture. The integration of SDNs into ULFC has been discovered to enhance its ability to withstand the penetration of chloride ions. The ULFC mixtures containing SDNs exhibited reduced values of the chloride diffusion coefficient when compared to the control ULFC mixture. The chloride diffusion coefficient of the control ULFC mixture was measured and documented at 3.82×10^{-13} m^2/s. By including various percentages of SDNs (0.5%, 1.0%, 1.5%, 2.0%, and 2.5%), the chloride diffusion coefficient demonstrated reductions of 3.93%, 13.87%, 28.53%, 36.13%, and 41.63%, respectively. The incorporation of SDNs in the ULFC mixtures has been found to enhance several fundamental properties, including the increased porosity, larger tortuosity, and a higher quantity of the solidified CSH gel. These improvements have proven to be crucial in mitigating the rate at which chlorides penetrate the ULFC material. Accordingly, the microstructure of ULFC is being densified as cement hydrates and progresses. In Fig. 13, the regression analysis of data acquired was executed to examine the relationship between the chloride diffusion coefficient with the pore volume of ULFC, average pore diameter, porosity, and water absorption. High correlations are shown between the chloride diffusion coefficient and pore volume, average pore diameter, porosity, and water absorption. The regression analyses in Fig. 13 reveal a notable linear association between the chloride diffusion coefficients and the various pore structure variables of ULFC. Moreover, the correlation coefficients consistently exceed 0.95, suggesting the substantial impact of the pore structure on the chloride diffusion coefficient of ULFC. The resistance to the chloride penetration of ULFC is directly proportional to the fineness of its pore structure. The parameter that gives the strongest correlation with the chloride diffusion coefficient is the pore volume of ULFC. The finding is consistent with the established trend in variations of the chloride diffusion, as described by Zhang and Li [123].

3.3. Thermal properties

Fig. 14(a–c) depicts the thermal properties' parameters of ULFC containing varying percentages of SDNs. The thermal conductivity, thermal diffusivity, and specific heat capacity of the ULFC mixtures containing 0.5%, 1.0%, 1.5%, 2.0%, and 2.5% of SDNs were determined and compared to those of the control mixture. In general, the integration

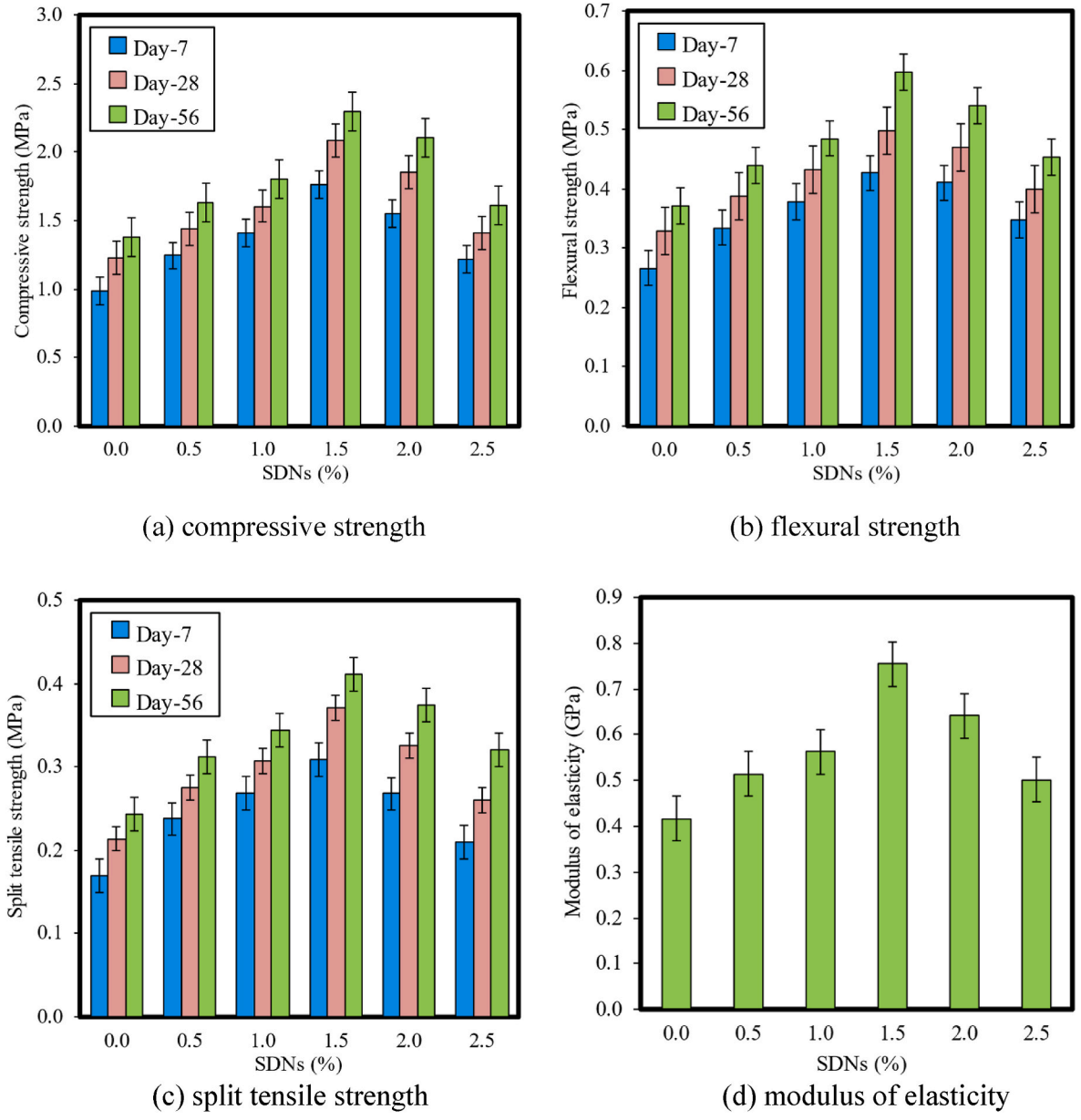

Fig. 16. Strength properties of ULFC containing varying percentages of SDNs.

of SDNs into ULFC has been found to increase the thermal properties' parameters of ULFC. In comparison to the control ULFC mixture, the ULFC mixtures containing SDNs indicated increased values of the thermal conductivity. The thermal conductivity of the control ULFC mixture was measured and documented at 0.129 W/mK. With the inclusion of 0.5%, 1.0%, 1.5%, 2.0%, and 2.5% of SDNs, the thermal conductivity illustrated enhancements of 5.43%, 8.53%, 11.63%, 13.18%, and 17.83%, respectively. Furthermore, the thermal diffusivity of ULFC followed the same trend as per the thermal conductivity. With an increase in the SDNs percentages in the ULFC mixtures, the thermal diffusivity increases as well. The thermal diffusivity of the control ULFC mixture was determined at 0.358 m^2/s. By integrating 0.5%, 1.0%, 1.5%, 2.0%, and 2.5% of SDNs, the thermal diffusivity displayed enhancements of 1.68%, 2.51%, 3.35%, 4.19%, and 5.59%, respectively. In contrast, the specific heat capacity of the ULFC mixtures decreased when the percentages of SDNs increased. The control ULFC mix recorded a specific heat capacity value of 862 J/kg K. With the presence of 0.5%, 1.0%, 1.5%, 2.0%, and 2.5% of SDNs, the specific heat capacity of ULFC decreased to 853 J/kg K, 852 J/kg K, 846 J/kg K, 839 J/kg K, and 834 J/kg K, respectively. The integration of SDNs in ULFC resulted in an increase in the thermal conductivity, demonstrating an enhancement in the modification of the pore structure. The observed phenomena can be attributed to the smaller pore size in the ULFC specimens with SDNs compared to the control ULFC specimen. This led to the increased heat conduction insulation. The comparable tendency was seen by microstructure analysis, as referenced in Subsection 3.5.2. The control specimen showed the existence of coalescing air bubbles. This occurrence has a possibility to reduce the heat conductivity due to the poor thermal conductivity of air [124].

Fig. 15 depicts the association between thermal characteristics parameters of ULFC including different proportions of SDNs. Significant relationships have been observed between the thermal characteristics' parameters, namely thermal conductivity, thermal diffusivity, and specific heat capacity, and proportions of SDNs. The regression studies present an important linear correlation between the parameters of the thermal characteristics and percentages of SDNs. Furthermore, it is seen that the correlation coefficients continuously transcend 0.97, indicating a significant influence of the percentages of SDNs in ULFC on the

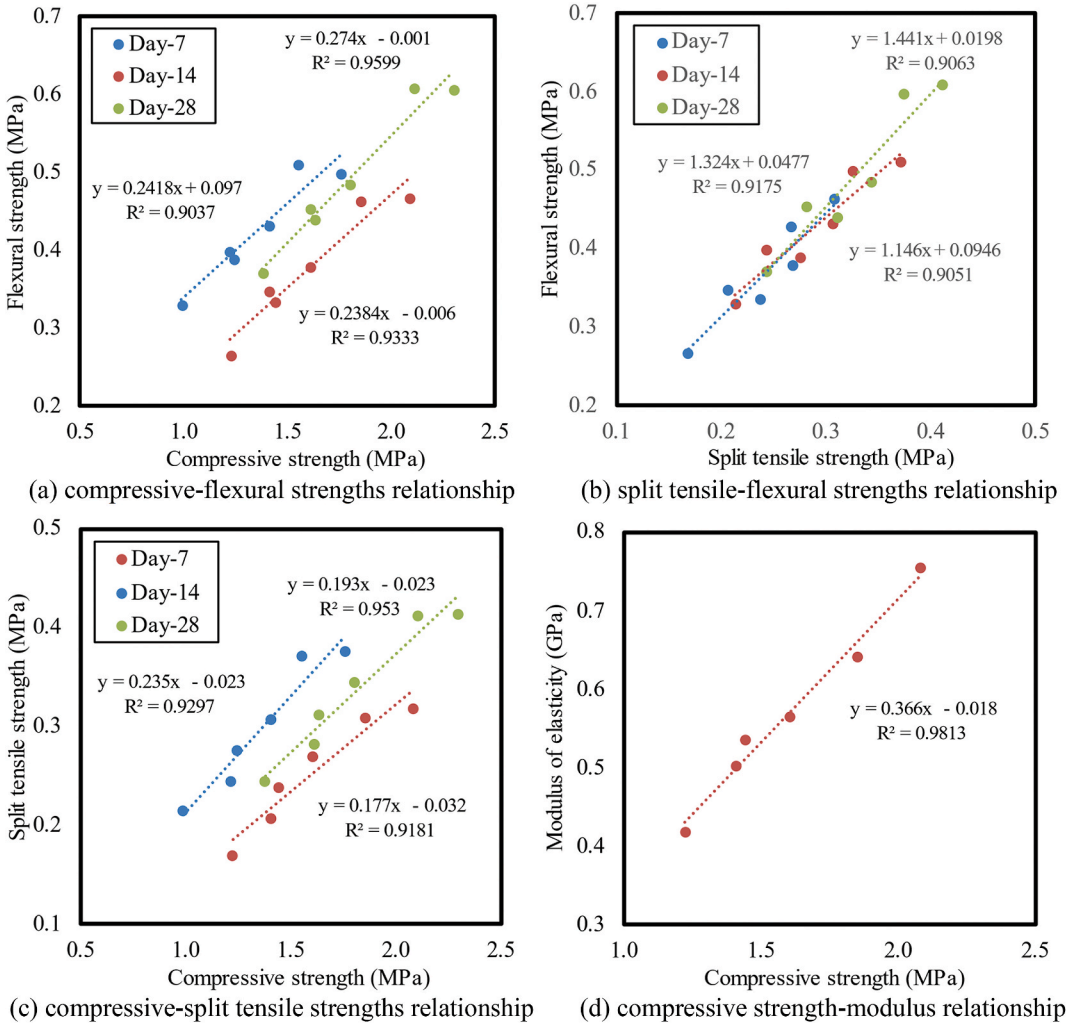

Fig. 17. Correlation between strength properties' parameters of ULFC containing varying percentages of SDNs.

parameters related to the thermal properties.

3.4. Mechanical properties

Fig. 16(a–d) illustrates the strength properties of ULFC containing varying percentages of SDNs at 7, 28, and 56 days. The compressive strength, flexural strength, split tensile strength, and modulus of elasticity of ULFC were considered. From Fig. 16, it can be clearly seen that the strength properties of ULFC increased dramatically with the inclusion of SDNs up to the ideal SDNs proportion of 1.5%. The strength properties started to decrease when the percentage of SDNs was raised to 2.0%.

The compressive strengths of the ULFC mixes with 0.5%, 1.0%, 1.5%, 2.0%, and 2.5% of SDNs were measured and compared to those of the control ULFC sample. With reference to Fig. 16(a), the compressive strength values at 7, 28, and 56 days were 0.99 MPa, 1.22 MPa, and 1.38 MPa, respectively. With the addition of 0.5%, 1.0%, 1.5%, 2.0%, and 2.5% of SDNs, the compressive strength of ULFC increased by 25.25%, 42.42%, 77.78%, 56.57%, and 23.23%, by 18.03%, 31.15%, 70.49%, 51.64%, and 15.57%, and by 18.12%, 30.43%, 66.67%, 52.90%, and 16.67%, respectively, at 7, 28, and 56 days. The significant increase in the compressive strength observed in ULFC blended with SDNs might be attributed to the accelerated consumption of calcium hydroxide that was generated during the hydration of cement. This phenomenon was particularly pronounced at the early stages of hydration, owing to the high reactivity of SDNs. Consequently, the process of the cement hydration was expedited, leading to the formation of a greater number of reaction products. Furthermore, the production of additional stiffening gel has the potential to enhance the limitations associated with the dispersion of SDNs. Moreover, SDNs facilitate the replenishment of particle packing density in the blended cement, resulting in a decrease in the volume of bigger pores within the cement paste [114]. In addition, SDNs reduced the volume of larger pores in the cement paste by recovering the particle packing density of the blended cement. Even though the recorded compressive strength started to decrease beyond the optimal SDNs percentage of 1.5%, but the values at 2.0% and 2.5% of SDNs were still higher than those of the control ULFC specimen. The observed effect can be attributed to the greater quantity of SDNs in the mixture compared to the necessary amount for reacting with the released lime throughout the phase of hydration. Consequently, an excessive amount of silica was leached out, resulting in a reduction of the compressive strength. Although SDNs were present in the cementitious matrix of ULFC, they did not influence the compressive strength of the composites.

As displayed in Fig. 16(b), the flexural strength values were 0.27 MPa, 0.33 MPa, and 0.37 MPa, respectively, at 7, 28, and 56 days. It was found that by adding 0.5%, 1.0%, 1.5%, 2.0%, and 2.5% of SDNs to ULFC, its flexural strength increased by 22.22%, 40.74%, 59.26%, 51.85%, and 29.63%, by 18.18%, 30.30%, 51.51%, 42.42%, and 21.21%, and by 18.92%, 29.73%, 62.16%, 45.95%, and 21.62%, respectively, at 7, 28, and 56 days. The increased flexural strength can be attributed to the accelerated pozzolanic reaction of SDNs when

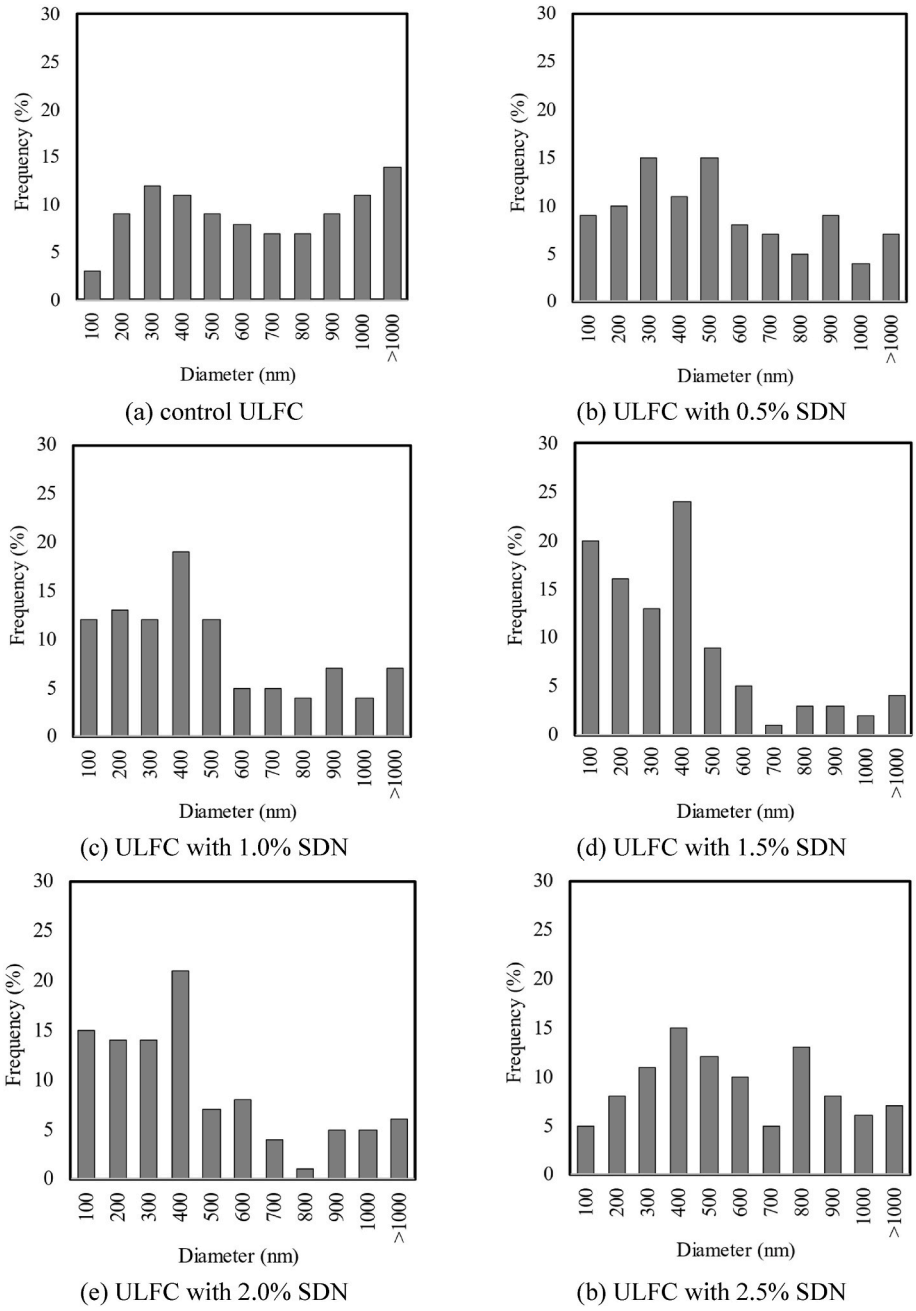

Fig. 18. Pore distributions of ULFC containing varying percentages of SDNs.

exposed to calcium hydroxide, resulting in a more compact morphology. Furthermore, the utilisation of SDNs could quicken the process of the hydration of tricalcium silicate clinker phase. This can be attributed to the substantial and highly responsive surface area of SDNs [118]. Nevertheless, the flexural strength demonstrated a marginal decline as the replacement amount approached 1.5%. Consequently, the increased incorporation of SDNs in ULFC did not result in the enhanced flexural strength, possibly due to the inadequate dissemination of the SDNs particles within the mixture. SDNs exhibited a notable inclination towards clustering owing to their increased surface energy. The distribution of SDNs throughout ULFC plays a crucial role in determining the efficacy of the composites.

Based on Fig. 16(c), the split tensile strength values at 7, 28, and 56 days were 0.17 MPa, 0.21 MPa, and 0.24 MPa, respectively. At 7, 28, and 56 days, the split tensile strength of ULFC increased by 41.18%, 58.82%, 82.35%, 58.82%, and 23.54%, by 33.33%, 47.62%, 76.19%, 57.14%, and 23.81%, and by 29.17%, 41.67%, 70.83%, 54.17%, and 33.33%, respectively, with the addition of 0.5%, 1.0%, 1.5%, 2.0%, and 2.5% of SDNs. The use of SDNs in ULFC for enhancing the split tensile strength is crucial because of their substantial reactivity during the initial phases.

As was observed for the compressive and flexural strengths, when an excessive amount of SDNs is introduced into the mixture, they are not evenly distributed within ULFC. As a result, weak regions occur in ULFC due to the formation of agglomerates thus reducing the split tensile strength of ULFC. Hence, the process of breaking down SDNs is of greatest significance to attain composite materials that exhibit enhanced characteristics [12]. Furthermore, it is possible that the quantities of SDNs present in the mixtures surpassed the necessary amount for the consumption of calcium hydroxide. However, the extra quantity of SDNs did not aid in the improvement of the compressive strength.

According to Fig. 16(d), the modulus of elasticity of ULFC improved dramatically with the inclusion of SDNs. At 7, 28, and 56 days, the

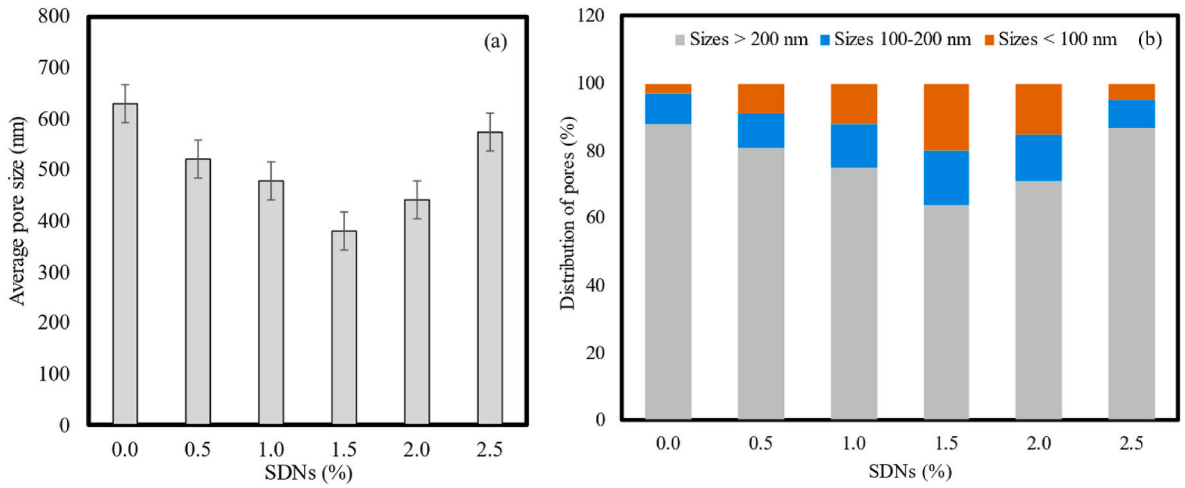

Fig. 19. ULFC pore size and distributions containing varying percentages of SDNs: (a) average pore size, (b) pore distributions.

modulus of elasticity of ULFC increased by 21.43%, 33.33%, 78.57%, 52.38%, and 19.05%, respectively. The utilisation of SDNs has been found to enhance the stability of ITZ. This improvement can be attributed to the formation of smaller and firmer CSH gel, which provided better rigidity thus enhanced the modulus of elasticity of ULFC. Additionally, the presence of SDNs led to an increased process of the hydration of the cement paste.

Fig. 17(a–d) depicts the correlation between the strength properties of SDNs. There have been notable associations identified among the mechanical strength parameters. The regression analyses in Fig. 17(a–d) show a significant linear relationship between the strength properties. Moreover, it is observed that the correlation coefficients consistently exceed 0.90, suggesting a substantial impact of the proportions of SDNs in ULFC on the mechanical characteristics such as the compressive strength, modulus of elasticity, split tensile strength, and flexural strength.

3.5. Microstructural properties

3.5.1. Pore distributions

The distribution of pore diameters in the matrix of ULFC is illustrated in Fig. 18(a–f), displaying the incorporation of SDNs as an additive throughout the range of 0.0%–2.5%. The findings of the study revealed a distinct alteration in the distribution of pore sizes in the ULFC mixes as the SDNs percentages changed. The ULFC specimens containing SDNs at percentages of 0.5%, 1.0%, and 1.5% demonstrated a reduction in the overall number of big pores measuring 500 nm and greater, in comparison to the control ULFC specimen. This was uncovered by the findings of the analysis of the average pore diameters, which are presented in Fig. 19(a). The pore sizes of the ULFC mixes added with 0.5%, 1.0%, 1.5%, 2.0%, and 2.5% were 630 nm, 521 nm, 480 nm, 380 nm, 443 nm, and 575 nm, respectively. This occurrence can be ascribed to the function of SDNs in decreasing the pore size via the pozzolanic response and the generation of the supplementary gel, hence mitigating the growth of the pore size [112]. This finding aligns with the outcomes of the mechanical properties of ULFC.

Addition of SDNs to the cementitious system results in the closely packed structure of the cementitious matrix and increase in the concrete matrix density by fillers, which improves the strength characteristics [115]. In accordance with the results of Fig. 19(b), it is evident that an increase in the percentage of SDNs leads to a consistent decrease in the volume of pores exceeding 200 nm in the specimens. This trend persists until reaching an optimal SDN percentage of 1.5%. This observation indicates an enhancement in the packing density of ULFC and a refinement in the pore structure. The integration of SDNs into the compositions reduced the overall porosity. The findings also revealed that the utilisation of the ULFC mixture containing 1.5% of SDNs exhibited the highest percentage of pore diameters measuring less than 100 nm. This phenomenon may be attributed to the interference of the capillary pores resulting from the increased production of the CSH gel [116].

This study shows that using SDNs in the ULFC mixtures at percentages ranging from 0.5% to 1.5% improved the compressive, flexural, and split tensile strengths, as well as modulus of elasticity, in comparison to the control ULFC mixture. In contrast, raising the SDNs percentages to 2.0% and 2.5% yielded a corresponding augmentation in the proportion of pores exhibiting a size of 500 nm and above. The observed conditions might potentially be attributed to the dispersion of cement, resulting in the weakening of the ULFC matrix. This deterioration, consequently, may have aided the creation of both big pores and irregular large pores, as visually depicted in the SEM images presented in Fig. 20(a–f). The stated issues agree with the findings of the strength properties tests conducted in this study. The test results reduced the strength of ULFC when replacement rates of 2.0% and 2.5% were employed.

3.5.2. SEM analysis

Fig. 20(a–f) displays the SEM images of the ULFC specimens that include the SDNs percentages that range from 0.0% to 2.5%. The pores' diameters and distribution inside the ULFC cementitious matrix can be more clearly visualised because of the significant details provided by the SEM images. In SEM of the control specimen illustrated in Fig. 20(a)–a diversified distribution of pores that indicated a large amount of variance in size and irregularities was seen. The incorporation of SDNs led to a further densification in the microstructure and to a reduction in the capillary porosity of the ULFC mixtures. In comparison to the control ULFC specimen, the microstructures of the ULFC mixes with 1.0% and 1.5% of SDNs were very dense (Fig. 20(b and c)), and small and micropores were observed. These samples demonstrate a reduction in larger calcium hydroxide structures (reduction in the larger dark space with introduction of SDNs is noted from the SEM images), which are transformed into smaller, more stable CSH structures. When compared to the control sample, it shows a more uniform and filled structure. With the presence of SDNs in ULFC, it was revealed that the amount of portlandite can be effectively reduced, leading to an improved microstructure of ITZ between sand and paste [119]. The control ULFC specimens displayed an insufficient bond between sand and paste (Fig. 20(a)), whereas the ULFC specimens with 1.5% of SDNs gave a perfect bond between sand and paste (Fig. 20(c)). As SDNs were able to bridge the small cracks in the cement paste, they contributed to the local toughening of ULFC, increasing its strength and decreasing its

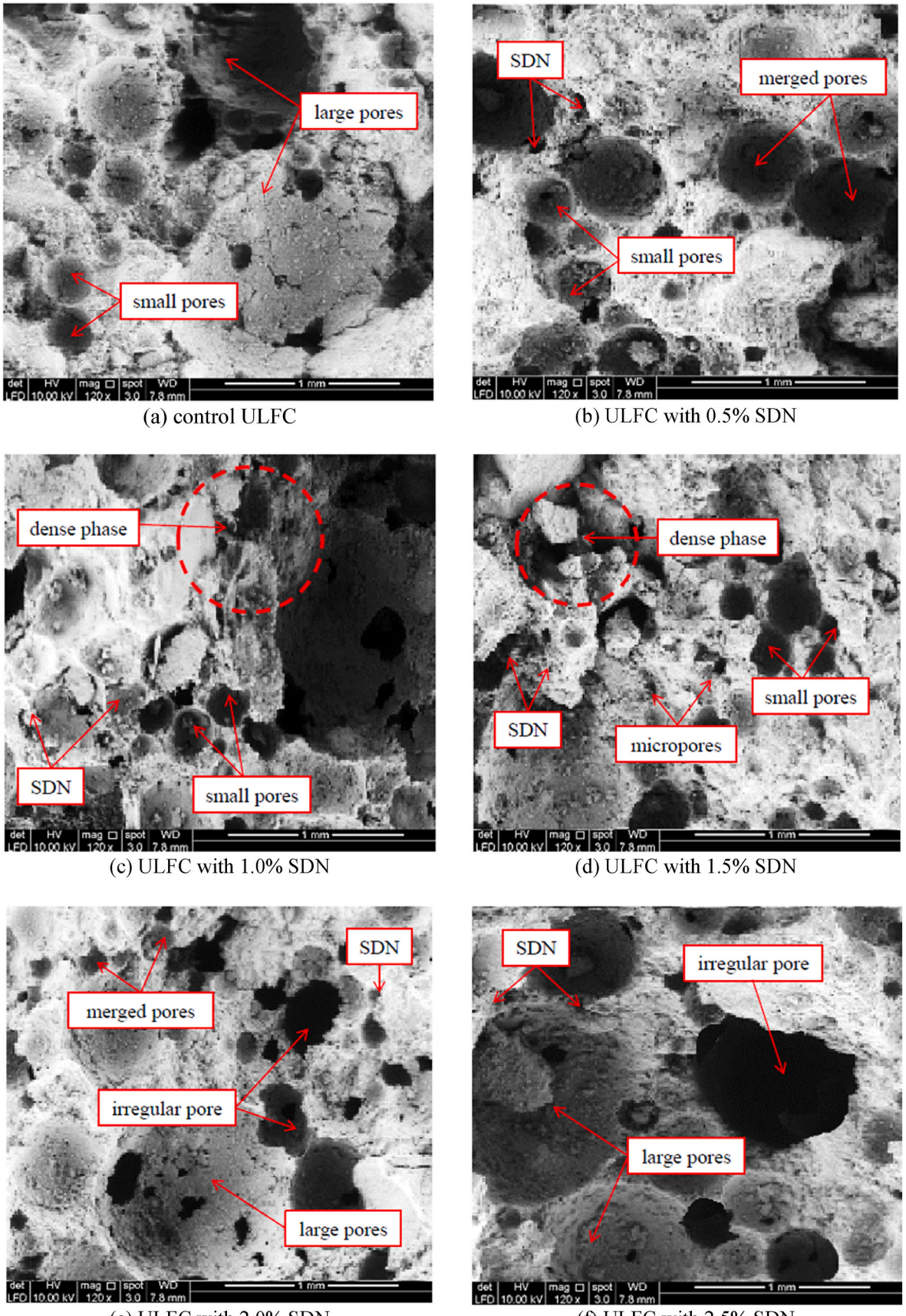

Fig. 20. Morphology of ULFC mixes containing different percentages of SDNs.

permeability. The inclusion of 2.0% of SDNs resulted in a SEM analysis revealing a more cohesive microstructure inside the composite material, as depicted in Fig. 20(d). This microstructure exhibited a notable absence of cavities and cracks. Nevertheless, the presence of micropores was seen, and it was noted that the diameter of the small pores was greater compared to the specimens containing 1.5% of SDNs. In contrast, an increase in the percentage of SDNs to 2% resulted in a growth of the diameter of the pores (Fig. 20(e)). The microstructural analysis of the ULFC samples containing 2.5% of SDNs revealed a higher level of porosity, characterised by a predominance of irregular forms (Fig. 20 (f)). The observed phenomena can be ascribed to the impact of dispersion on cement, leading to a microstructure characterised by the reduced density and increased porosity [113]. The finding was corroborated by the results obtained from the mechanical properties tests carried out within the scope of this study. These results indicate a decrease in the strength parameters when utilising the SDNs percentages of 2.0% and 2.5% in comparison to the ULFC specimen with the presence of 1.5% of SDNs.

4. Conclusions

Considering the recent emergence of nanoscale materials into the concrete manufacturing sector, it is imperative to put forward comprehensive findings from studies to enhance the understanding of the impact of these substances on the characteristics of concrete. This study assessed the fresh state, mechanical, microstructural, transport, and thermal properties of ULFC using various percentages of SDNs ranging from 0.0% to 2.5%. The investigation's findings are detailed below:

- The incorporation of SDNs into ULFC resulted in a substantial enhancement of their mechanical properties. In comparison to the control ULFC, the inclusion of 1.5% of SDNs led to significant improvements in several strength properties. Specifically, the 28-day compressive strength illustrated an increase of up to 70.49%, the splitting strength exhibited an increase of up to 76.19%, and the flexural strength demonstrated an increase of up to 51.51%. This SDNs percentage was determined to be the ideal level to achieve the intended outcomes. A 2.0% addition of SDNs, on the other hand, provided some improvements in the mechanical properties but was below the ideal percentage.
- Increasing SDNs to 2.5% increased the initial and final setting times by 27.34% and 14.74%, respectively.
- The greater the increase in SDNs was, the greater the increase in the density was.
- ULFC incorporating SDNs displayed higher thermal conductivity values compared to the control ULFC. The reduced pore size seen in the ULFC specimens with SDNs was identified as the cause of this occurrence, in contrast to the control ULFC specimen. As a result, there was a notable enhancement in the insulation of the heat conduction.
- The sorptivity, porosity, water absorption, intrinsic air permeability, and chloride diffusion of ULFC mixed with SDNs revealed significant enhancement as the percentage of SDNs raised from 1.5% to 2.5%.
- A noticeable modification in the distribution of pore diameters was witnessed in the ULFC mixes as the percentages of SDNs were adjusted. The ULFC specimens, which incorporated SDNs at percentages of 0.5%, 1.0%, and 1.5%, indicated a decrease in the total count of large voids with a size of 500 nm or larger, as compared to the control ULFC specimen. This can be explained by the effect of SDNs in reducing the size of pores through the pozzolanic reaction and the creation of the extra gel, which inhibits the pores from growing.
- The results of this study emphasise the potential benefits of integrating SDNs into ULFC, offering possibilities for improving the overall strength performances of ULFC.

ULFC is thus can be utilised in a variety of construction projects owing to its distinctive characteristics, including low self-weight, high flowability, self-compacting nature, and easy manufacturing process. It is ideal for void filling and insulating materials, whereas high-density LWFC has been used in structural purposes. ULFC may additionally be employed for making blocks and prefabricated panels, fire insulating materials, road subbase, shock absorption barriers, and soil stabilisation. Additionally, ULFC is recommended for utilisation in locations that are subject to mild climatic conditions, such as regions with moderate rainfall. Water can infiltrate the voids in concrete, where there is low absorption.

Declaration of competing interest

The authors declare that they have no known competing financial interests or personal relationships that could have appeared to influence the work reported in this article.

Acknowledgement

The authors would like to thank the Ministry of Higher Education, Malaysia, for the financial assistance to this research work through the Fundamental Research Grant Scheme (Grant Reference Number: FRGS/1/2022/TK01/USM/02/3).

List of Abbreviations

CSH	Calcium silicate hydrate
HPC	High-performance concrete
ITZ	Interfacial transition zone
LWFC	Lightweight foamed concrete
MIP	Mercury intrusion porosimetry
SDNs	Silicon dioxide nanoparticles
SEM	Scanning electron microscopy
TEM	Transmission electron microscopy
ULFC	Ultra-lightweight foamed concrete

References

[1] Shaikh FUA, Supit SWM, Sarker PK. A study on the effect of nano silica on compressive strength of high volume fly ash mortars and concretes. Mater Des 2014;60:433–42. https://doi.org/10.1016/j.matdes.2014.04.025.
[2] Celik K, Meral C, Petek Gursel A, Mehta PK, Horvath A, Monteiro PJM. Mechanical properties, durability, and life-cycle assessment of self-consolidating concrete mixtures made with blended Portland cements containing fly ash and limestone powder. Cem Concr Compos 2015;56:59–72. https://doi.org/10.1016/J.CEMCONCOMP.2014.11.003.
[3] Li H, Zhang MH, Ou JP. Abrasion resistance of concrete containing nano-particles for pavement. Wear 2006;260(11–12):1262–6. https://doi.org/10.1016/j.wear.2005.08.006.
[4] Singh LP, Ali D, Sharma U. Studies on optimization of silica nanoparticles dosage in cementitious system. Cem Concr Compos 2016;70:60–8.
[5] Sharma VP, Sharma U, Chattopadhyay M, Shukla VN. Advance applications of nanomaterials - a review. Mater Today Proc 2018;5:6376–80.
[6] Morsy MS, Alsayed SH, Aqel M. Hybrid effect of carbon nanotube and nanoclay on pysicho-mechanical properties of cement mortar. Construct Build Mater 2011;25:145–9.
[7] Chenglong Z, Yu C. The effects of nanosilica on concrete properties - a review. Nanotechnol Rev 2019;8:562–72.
[8] Mohammad RA, Saeed RZ. Synthesis of zinc oxide nanoparticles and their effect on the compressive and setting time of self compacted concrete paste as cementitious composites. Int J Mol Sci 2012;13:4340–50.
[9] Khaloo A, Mobini MH, Hosseini P. Influence of different types of nanosilica on the properties of high performance concrete. Construct Build Mater 2016;113:188–201.
[10] Lateef A, Azeez MA, Asafa TB, Yekeen TA, Akinboro A, Oladipo IC, Azeez L, Ajibade SE, Ojo SA, Guegium-Kana EB, Beukes LS. Biogenic synthesis of silver nanoparticles using a pod extract of cola nitida: antibacterial and antioxidant activities and application as a paint additive. J Taibah Univ Sci 2016;10:551–62.
[11] Gajanan K, Tijare SN. Application of nanomaterials. Mater Today Proc 2018;5:1093–6.
[12] Mydin MAO. Thin-walled steel enclosed lightweight foamcrete: a novel approach to fabricate sandwich composite. Aust J Basic and Appl Sci 2011;5(12):1727–33.

[13] Jo BW, Kim CH, Tae GH, Park JB. Characteristics of cement mortar with nanosilica particles. Construct Build Mater 2007;21:1351–5.
[14] Mahender B, Ashbok B. Effects of nano silica on the compressive strength of concrete. Int J Professional Eng Stud 2017;3(2):222–6.
[15] Maglad AM, Mydin MAO, Datta SD, Tayeh BA. Assessing the mechanical, durability, thermal and microstructural properties of sea shell ash based lightweight foamed concrete. Construct Build Mater 2023;402:133018.
[16] Alyami M, Othuman Mydin MA, Zeyad AM, Majeed SS, Tayeh BA. Influence of wastepaper sludge ash as partial cement replacement on the properties of lightweight foamed concrete. J Build Eng 2023;79:107893.
[17] Zamzani N, Abdul Ghani AN. Experimental data on compressive and flexural strengths of coir fibre reinforced foamed concrete at elevated temperatures. Data Brief 2019;25:104320.
[18] Mohd Nawi MN, Lee A. Supply chain management (SCM): disintegration team factors in Malaysian Industrialised Building System (IBS) construction projects. Int J Supply Chain Manag 2018;7(1):140–3.
[19] Celik AI, Tunc U, Bahrami A. Use of waste glass powder toward more sustainable geopolymer concrete. J Mater Res Technol 2023;24:8533–46.
[20] Mohamed Shajahan MF, Ganesan S. Laboratory investigation on compressive strength and micro-structural features of foamed concrete with addition of wood ash and silica fume as a cement replacement. In: MATEC Web of Conferences, 17; 2014, 01004.
[21] Phius AF. Potential of green construction in Malaysia: industrialised building system (IBS) vs traditional construction method. In: E3S Web of Conferences, 3; 2014, 01009.
[22] Ganesan S. Performance of polymer modified mortar with different dosage of polymeric modifier. In: MATEC Web of Conferences, 15; 2014, 01039.
[23] Serri E, Suleiman MZ. The influence of mix design on mechanical properties of oil palm shell lightweight concrete. J Mater Environ Sci 2015;6(3):607–12.
[24] Sani NM. Imperative causes of delays in construction projects from developers' outlook. In: MATEC Web of Conferences, 10; 2014, 06005.
[25] Sahidun NS. Compressive, flexural and splitting tensile strengths of lightweight foamed concrete with inclusion of steel fibre. Jurnal Teknologi 2015;75(5): 45–50.
[26] Ji T. Preliminary study on the water permeability and microstructure of concrete incorporating nano-SiO2. Cement Concr Res 2005;35:1943–7.
[27] Chen WF, Lv G, Hu WM, Li DJ, Chen SN, Z X. Synthesis and applications of graphene QuantumDots: a review. Nanotechnol Rev 2018;7(2):157–85.
[28] Aslam A, Jamil MK, Gao W, Nazeer W. Topological aspects of some dendrimer structures. Nanotechnol Rev 2018;7(2):123–39.
[29] Mosstafa K, Massoud G, Ali M. Cobalt ferrite nanoparticles (CoFe2O4 Mnps) as catalyst and support: magnetically recoverable nanocatalysts in organic synthesis (Nano-composites). Nanotechnol Rev 2018;7(1):43–68.
[30] Kandasamy G, Annenkov VV, Krishnan UM. Nanoimmunotherapy-cloaked defenders to breach the cancer fortress. Nanotechnol Rev 2018;7(4):317–40.
[31] Ali A, Phull AR, Zia M. Elemental zinc to zinc nanoparticles: is Zno Nps crucial for life? Synthesis, toxicological, and environmental concerns (can be related with nano-bio). Nanotechnol Rev 2018;7(5):413–41.
[32] Chen C, Hou X, Si JH. Carbohydrate-protein interactions characterized by dual polarization hybrid plasmonic waveguide. Nanotechnol Rev 2018;7(1):11–8.
[33] Scott A, Vadalasetty KP, Chwalibog A. Copper nanoparticles as an alternative feed additive in poultry diet: a review (Nano-bio). Nanotechnol Rev 2018;7(1):69–93.
[34] Li G. Properties of high-volume fly ash concrete incorporating nano-SiO2. Cement Concr Res 2004;34:1043–9.
[35] Li H, Xiao HG, Yuan J, Ou JP. Microstructure of cement mortar with nanoparticles. Compos B 2004;35:185–9.
[36] Naji Givi A, Abdul Rashid S, Aziz FNA, Salleh MAM. The effects of lime solution on the properties of SiO_2 nanoparticles binary blended concrete. Compos. Part B Eng. 2011;42(3):562–9.
[37] Sureshkumar MP, Visakan M, Student PG. Experimental investigation on applications of nanomaterials in concrete. Int. J. Struct. Civ. Eng. Res. 2017;3(2): 1–9 [Online]. Available,, https://www.ijirset.com.
[38] Ying JW, Zhou B, Xiao JZ. Pore structure and chloride diffusivity of recycled aggregate concrete with nano-SiO_2 and nano-TiO_2. Construct Build Mater 2017; 150:49–55.
[39] Eskandari H, Vaghefi M, Kowsari K. Investigation of mechanical and durability properties of concrete influenced by hybrid nano silica and micro zeolite. Procedia Mater. Sci. 2015;11:594–9.
[40] He K, Chen Y, Xie WT. Test on axial compression performance of nano-silica concrete-filled angle steel reinforced GFRP tubular column. Nanotechnol Rev 2019;8:523–38.
[41] M. Khanzadi, M. Tadayon, H. Sepehri and M. Sepehri, Influence of nano-silica particles on mechanical properties and permeability of concrete. Second international conference on sustainable construction material and technologies..
[42] Ma QY, Zhu Y. Experimental research on the microstructure and compressive and tensile properties of nano-SiO_2 concrete containing basalt fibers. Undergr Space 2017;2(3):175–81.
[43] Makarova NV, Potapov VV, Kozin AV, Chusovitin EA, Amosov AV, Nepomnyashiy AV. Influence of hydrothermal nanosilica on mechanical properties of plain concrete. 744 744 KE Key Eng Mater 2017:126–30.
[44] Sobolev K, Ferrara M. How nanotechnology can change the concrete world – Part 1. Am Ceram Soc Bull 2005;84:16–20.
[45] Jagadesh P, Karthik Prabhu T, Moutassim Charai, Hakeem IY, Madenci E, Ozkilic YO. A potential review on the influence of nanomaterials on the mechancial properties of high strength concrete. Steel Compos Struct 2023;48(6): 649–66. https://doi.org/10.12989/scs.2023.48.6.649.
[46] Krishnan P, Zhang MH, Cheng Y, Riang DT, Yu LE. Photocatalytic degradation of SO_2 using TiO_2-containing silicate as a building coating material. Construct Build Mater 2013;43:197–202.
[47] Jagadesh P, Nagarajan V, Karthik Prabhu T, Karthik Arunachalam K. Effect of nano titanium di oxide on mechanical properties of fly ash and ground granulated blast furnace slag based geopolymer concrete. J Build Eng 2022;61:105235. https://doi.org/10.1016/j.jobe.2022.105235.
[48] Le JL, Du H, Pang SD. Use of 2-D Graphene Nanoplatelets (GNP) in cement composites for structural health evaluation. Compos B 2014;67:555–63.
[49] Du H, Quek ST, Pang SD. Smart multifunctional cement mortar containing graphite nanoplatelet. In: Lynch JP, Yun CB, Wang KW, editors. Sensors and smart structures technologies for civil, mechanical, and aerospace system. San Diego; 2013.
[50] Konsta-Gdoutos MS, Metaxa ZS, Shah SP. Highly dispersed carbon nanotube reinforced cement based materials. Cement Concr Res 2010;40:1052–9.
[51] Metaxa ZS, Konsta-Gdoutos MS, Shah SP. Carbon nanofiber cementitious composites: effect of debulking procedure on dispersion and reinforcing efficiency. Cem Concr Compos 2013;36:25–32.
[52] Mydin MAO, Jagadesh P, Bahrami A, Dulaimi A, Ozkilic YO, Abdullah MMAB, Jaya RP. Use of calcium carbonate nanoparticles in production of nano-engineered foamed concrete. J Mater Res Technol 2023;26:4405–22. https://doi.org/10.1016/j.jmrt.2023.08.106.
[53] Kawashima S, Hou P, Corr DJ, Shah SP. Modification of cement based materials with nanoparticles. Cem Concr Compos 2013;36:8–15.
[54] Li H, Xiao H, Yuan J, Ou J. Microstructure of cement mortar with nano-particles. Compos: Part B 2004;35:185–9.
[55] Liu M, Tan HB, He XY. Effects of nano-SiO_2 on early strength and microstructure of steam-cured high volume fly ash cement system. Construct Build Mater 2019; 194:350–9.
[56] Hosseini P, Booshehrian A, Madari A. Developing concrete recycling strategies by utilization of nano-SiO_2 particles. Waste Biomass Valorization 2011;2(3):347–55.
[57] Singh LP, Goel A, Bhattachharyya SK, Ahalawat S, Sharma U, Mishra G. Effect of morphology and dispersibility of silica nanoparticles on the mechanical behaviour of cement mortar. Int. J. Concr. Struct. Mater. 2015;9(2):207–17.
[58] Li QH, Gao X, Xu SL. Multiple effects of nano-SiO2 and hybrid fibers on properties of high toughness fiber reinforced cementitious composites with high-volume fly ash. Cem Concr Compos 2016;72:201–12.
[59] Jo BW, Kim CH, Lim JH. Characteristics of cement mortar with nano-silica particles. ACI Mater J 2007;104(4):404–7.
[60] Zhang MH, Islam J. Use of nano-silica to reduce setting time and increase early strength of concretes with high volume fly ash or slag. Construct Build Mater 2012;29:573–80.
[61] Phoo-ngernkham T, Chindaprasirt P, Sata V, Hanjitsuwan S. The effect of adding nano-silica and nano-alumina on properties of high calcium fly ash geopolymer cured at ambient temperature. Mater Des 2014;55:58–65.
[62] Zhang BL, Tan HB, Shen WG, Xu GL, Ma BG, Ji XL. Nanosilica and silica fume modified cement mortar used as Surface Protection Material to enhance the impermeability. Cem Concr Compos 2018;92:7–17.
[63] Wang YS, Xu ZH, Wang JB, Zhou ZH, Du P, Cheng X. Synergistic effect of nano-silica and silica fumeon hydration properties of cement-based materials. J Therm Anal Calorim 2019:1–11.
[64] Prashanth R, Selvan SS, Balasubramanian M. Experimental investigation on durability properties of concrete added with nano silica. Rasayan J. Chem. 2019; 12(2):685–90.
[65] Liu R, Xiao HG, Liu JL, Guo S, Pei YF. Improving the microstructure of ITZ and reducing the permeability of concrete with various water/cement ratios using nano-silica. J Mater Sci 2019;54(1):444–56.
[66] Mohammed BS, Liew MS, Alaloul WS, Khed VC, Hoong CY, Adamu M. Properties of nano-silica modified pervious concrete. Case Stud Constr Mater 2018;8: 409–22.
[67] Flores I, Sobolev K, Torres-Martinez L, Cuellar E, Valdez P, Zarazua E. Performance of cement systems with nano-SiO_2 particles produced by using the sol–gel method. Transport Res Rec: J Transport Res Board 2010;2141:10–4.
[68] Erdem S, Hanbay S, Güler Z. Micromechanical damage analysis and engineering performance of concrete with colloidal nano-silica and demolished concrete aggregates. Construct Build Mater 2018;171:634–42. https://doi.org/10.1016/j.conbuildmat.2018.03.197.
[69] Li G. Properties of high-volume fly ash concrete incorporating nano-SiO_2. Cement Concr Res 2004;34(6):1043–9. https://doi.org/10.1016/j.cemconres.2003.11.013.
[70] Sivasankaran U, Raman S, Nallusamy S. Experimental analysis of mechanical properties on concrete with nano silica additive. J Nano Res 2019;57:93–104. https://doi.org/10.4028/www.scientific.net/JNanoR.57.93.
[71] Madani H, Bagheri A, Parhizkar T. The pozzolanic reactivity of monodispersed nanosilica hydrosols and their influence on the hydration characteristics of Portland cement. Cement Concr Res 2012;42:1563e1570.
[72] Ghafari E, Costa H, Júlio E, Portugal A, Durães L. The effect of nanosilica addition on flowability, strength and transport properties of ultra high performance concrete. Mater Des 2014;59:1–9.
[73] Jalal M, Pouladkhan A, Harandi OF, Jafari D. Comparative study on effects of Class F fly ash, nano silica and silica fume on properties of high performance self compacting concrete. Construct Build Mater 2015;94:90–104. https://doi.org/10.1016/j.conbuildmat.2015.07.001.
[74] Verma M, et al. Experimental analysis of geopolymer concrete : a sustainable and economic concrete using the cost estimation model. Adv Mater Sci Eng 2022; 2022:1–16.

[75] Upreti K, et al. Prediction of mechanical strength by using an artificial neural network and random forest algorithm. J Nanomater 2022;2022:1–12.
[76] Du H, Du S, Liu X. Effect of nano-silica on the mechanical and transport properties of lightweight concrete. Construct Build Mater 2015;82:114–22.
[77] Ai-khalaf MN, Yousift HA. Use of rice husk ash in concrete. Int J Cem Compos Lightweight Concr 1984;6(4):241–8.
[78] Güneyisi E, Gesoglu M, Azez OA, Öz HÖ. Effect of nano silica on the workability of self-compacting concretes having untreated and surface treated lightweight aggregates. Construct Build Mater 2016;115:371–80.
[79] Quercia C, Spiesz P, Husken G, Brouwers HJH. SCC modification by use of amorphous nano-silica. Cem Concr Compos 2014;45:69–81.
[80] Du H, Pang SD. Effect of colloidal nano-silica on the mechanical and durability performances of mortar. Key Eng Mater 2014;629:443–8.
[81] MS522. Portland cement (ordinary and rapid-hardening): Part 1 specification (second revision) – 709539. Malaysia: Department of Standards Malaysia; 2003.
[82] ASTM C33-03. Standard specification for concrete aggregates. American society for testing and materials. West Conshohocken, PA: ASTM International; 2003.
[83] BS EN 3148. Water for making concrete (including notes on the suitability of the water). London, UK: British Standards Institute; 1980.
[84] ASTM C796M-19. Standard test method for foaming agents for use in producing cellular concrete using preformed foam. American society for testing and materials. West Conshohocken, PA: ASTM International; 2019.
[85] Shaikh FUA, Supit SWM, Sarker PK. A study on the effect of nano silica on compressive strength of high volume fly ash mortars and concretes. Mater Des 2014;60:433e442.
[86] Sobolev K, Flores I, Torres- Martinez LM, Valdez PL, Zarazua E, Cuellar EL. Engineering of SiO_2 nanoparticles for optimal performance in nano cement based materials. NANOCON 2013;10:16e18.
[87] Singh LP, Bhattacharyya SK, Ahalawat S. Preparation of size controlled silica nanoparticles and its functional role in cementitious system. J Adv Concr Technol 2012;10:345e352.
[88] Berra M, Carassiti F, Mangialardi T, Paolini AE, Sebastiani M. Effects of nanosilica addition on workability and compressive strength of Portland cement pastes. Construct Build Mater 2012;35:666–75.
[89] Qing Y, Zenan Z, Deyu K, Rongshen C. Influence of nano-SiO_2 addition on properties of hardened cement paste as compared with silica fume. Construct Build Mater 2007;21:539–45.
[90] Mukharjee BB, Barai SV. Characteristics of mortars containing colloidal nano-silica. IJAER 2014;1:17–22.
[91] Qian J, Hou P, Wang K, Kawashima S, Kong D, Shah SP. Effects of colloidal nanoSiO2 on fly ash hydration. Cement Concr Compos 2012;34:1095–103.
[92] Heikal M, Aleem SA, Morsi WM. Characteristics of blended cements containing nano-silica. HBRC J 2013;9:243–55.
[93] ASTM C 230-97. Flow table for use in tests of hydraulic cement. American society for testing and materials. West Conshohocken, PA: ASTM International; 1997.
[94] BS EN 196-3. Methods of testing cement. Determination of setting times and soundness. London, UK: British Standards Institute; 2016.
[95] BS 12350-6. Testing fresh concrete Density. London, UK: British Standards Institute; 2019.
[96] BS EN 1881-122. Testing concrete Method for determination of water absorption. London, UK: British Standards Institute; 2020.
[97] ASTM C1403-15. Standard test method for rate of water absorption of masonry mortars. West Conshohocken, PA: ASTM International; 2015.
[98] Cabrera JG, Lynsdale CJ. A new gas permeameter for measuring the permeability of mortar and concrete. Mag Concr Res 1988;40(144):177–82.
[99] ASTM 1202-19. Standard test method for electrical indication of concrete's ability to resist chloride ion penetration. West Conshohocken, PA: ASTM International; 2019.
[100] ASTM C177-19. Standard test method for steady-state heat flux measurements and thermal transmission properties by means of the guarded-hot-plate apparatus. American society for testing and materials. West Conshohocken, PA: ASTM International; 2019.
[101] BS EN 12390-5. Testing hardened concrete. Flexural strength of test specimens. London, UK: British Standards Institute; 2019.
[102] BS EN 12390-6. Testing Hardened Concrete. Tensile splitting strength of test specimens. London, UK: British Standards Institute; 2009.
[103] BS EN 12390-3. Testing Hardened Concrete. Compressive strength of test specimens. London, UK: British Standards Institute; 2011.
[104] ASTM C469. Standard test method for static modulus of elasticity and Poisson's ratio of concrete in compression. American society for testing and materials. West Conshohocken, PA: ASTM International; 2002.
[105] ASTM D4404-18. Standard test method for determination of pore volume and pore volume distribution of soil and rock by mercury intrusion porosimetry. American society for testing and materials. West Conshohocken, PA: ASTM International; 2018.
[106] ISO 16700. Microbeam analysis — scanning electron microscopy — guidelines for calibrating image magnification. International Organization for Standardization; 2016.
[107] Bernal J, et al. Fresh and mechanical behavior of a self-compacting concrete with addition of nano-silica, silica fume and ternary mixtures. Construct Build Mater 2018;160:196–210.
[108] Durgun MY, Atahan HN. Rheological and fresh properties of reduced fine content self-compacting concretes produced with different particle sizes of nano SiO_2. Construct Build Mater 2017;142(2017):431–43.
[109] Mukharjee BB, Barai SV. Influence of Nano-Silica on the properties of recycled aggregate concrete. Construct Build Mater 2014;55:29–37.
[110] Abhilash PP, Nayak DK, Sangoju B, Kumar R, Kumar V. Effect of nano-silica in concrete; a review. Construct Build Mater 2021;278:122347. https://doi.org/10.1016/j.conbuildmat.2021.122347.
[111] Wang L, Zheng D, Zhang S, et al. Effect of nano-SiO_2 on the hydration and microstructure of Portland cement. Nanomaterials 2016;6. https://doi.org/10.3390/nano6120241.
[112] Said AM, et al. Properties of concrete incorporating nano-silica. Construct Build Mater 2012;36:838–44.
[113] Oltulu M, Sahin R. Pore structure analysis of hardened cement mortars containing silica fume and different nano-powders. Construct Build Mater 2014;53:658–64.
[114] Zahedi M, Ramezanianpour AA, Ramezanianpour AM. Evaluation of the mechanical properties and durability of cement mortars containing nanosilica and rice husk ash under chloride ion penetration. Construct Build Mater 2015;78:354–61.
[115] Yakovlev G, Grakhov V, Polyanskih I, Gordina A, Pudov I, Mohhamed A, Karpova E, Saraykina K, Saidova Z. Dispersion degree and its influence on structure of building materials. In: IOP Conference Series: Materials Science and Engineering, 471; 2019, 032003. https://10.1088/1757-899X/471/3/032003.
[116] Chithra S, Kumar SS, Chinnaraju K. The effect of Colloidal Nano-silica on workability, mechanical and durability properties of High Performance Concrete with Copper slag as partial fine aggregate. Construct Build Mater 2016;113:794–804.
[117] Wang D, Shi C, Wu Z, Wu L, Xiang S, Pan X. Effects of nanomaterials on hardening of cement–silica fume– fly ash-based ultra-high-strength concrete. Adv Cement Res 2016;28(9):555–66.
[118] Tobon JI, Payá J, Restrepo OJ. Study of durability of Portland cement mortars blended with silica nanoparticles. Construct Build Mater 2015;80:92–7.
[119] Abd Elrahman M, Chung SY, Sikora P, Rucinska T, Stephan D. Influence of nanosilica on mechanical properties, sorptivity, and microstructure of lightweight concrete. Materials 2019;12(19):3078.
[120] Arif M, Hasan SD, Siddiqui S. Effect of nano silica on strength and permeability of concrete Author links open overlay panel. Mater Today Proc 2023.
[121] Abdalla JA, Thomas BS, Hawileh RA, Yang J, Jindal BB, Ariyachandra E. Influence of nano-TiO_2, nano-Fe_2O_3, nanoclay and nano-$CaCO_3$ on the properties of cement/geopolymer concrete. Clean. Mater. 2022;4(173).
[122] Barbhuiya GH, Moiz MA, Hasan SD, Zaheer MM. Effects of the nano-silica addition on cement concrete: a review. Mater Today Proc 2020;32(4):560–6.
[123] Zhang MH, Li H. Pore structure and chloride permeability of concrete containing nano-particles for pavement. Constr. Build. Mater. 2011;252.
[124] Hassan NM, Othuman Mydin MA, Awang H. Investigation of thermal, mechanical and transport properties of ultra-lightweight foamed concrete (ULFC) strengthened with alkali treated banana fibre. J. Adv. Res. Fluid Mech. Therm. Sci. 2021;86(1):123–39.